CHAPTER III
ATTENUATION MODELS

In the pursuit of identifying the most appropriate attenuation model for Bangkok, eighteen attenuation models are selected and subjected to further analysis. Basically, the criterion for the selection is based on previous researches in the region as mentioned in literature review. Some of the models in recent publications are also taken into account.

3.1   Theoretical Background

Attenuation relationships are predictive equations for parameters like peak ground acceleration, peak ground velocity and spectral acceleration that decrease with increasing distance. These equations provide probabilistic descriptions of the level of ground shaking as a function of the earthquake and site parameters (Raoof *et al.*, 1999). The use of this relation paves the way towards a fundamental step in earthquake hazard assessment which is the estimation of probable ground motion for engineering design.

The general functional form of attenuation relations is given in Equation 3.1 (Sellami, S., 2000).

$$\ln(Y) = \ln(b_1) + \ln f_1(M) + \ln f_2(R) + \ln f_3(M,R) + \ln f_4(P_i) + \ln(\varepsilon) \qquad (3.1)$$

where

Y = ground motion parameter;

b_1 = scaling factor;

$f_1(M)$ = function of magnitude;

$f_2(R)$ = function of distance;

$f_3(M, R)$ = possible joint function between magnitude and distance;

$f_4(P_i)$ = other variables representing possible source and site effects; and

ε = random error term that accounts for uncertainties in Y.

The development of attenuation relationship entails well-documented account of earthquake events that best represents the conditions of the site. An overview of the general procedures that are typically followed to come up with this ground motion database is depicted in Figure 3.1. These selection criteria are adopted from the procedures suggested by Douglas (2003) as guidelines in deriving ground motion estimation equations.
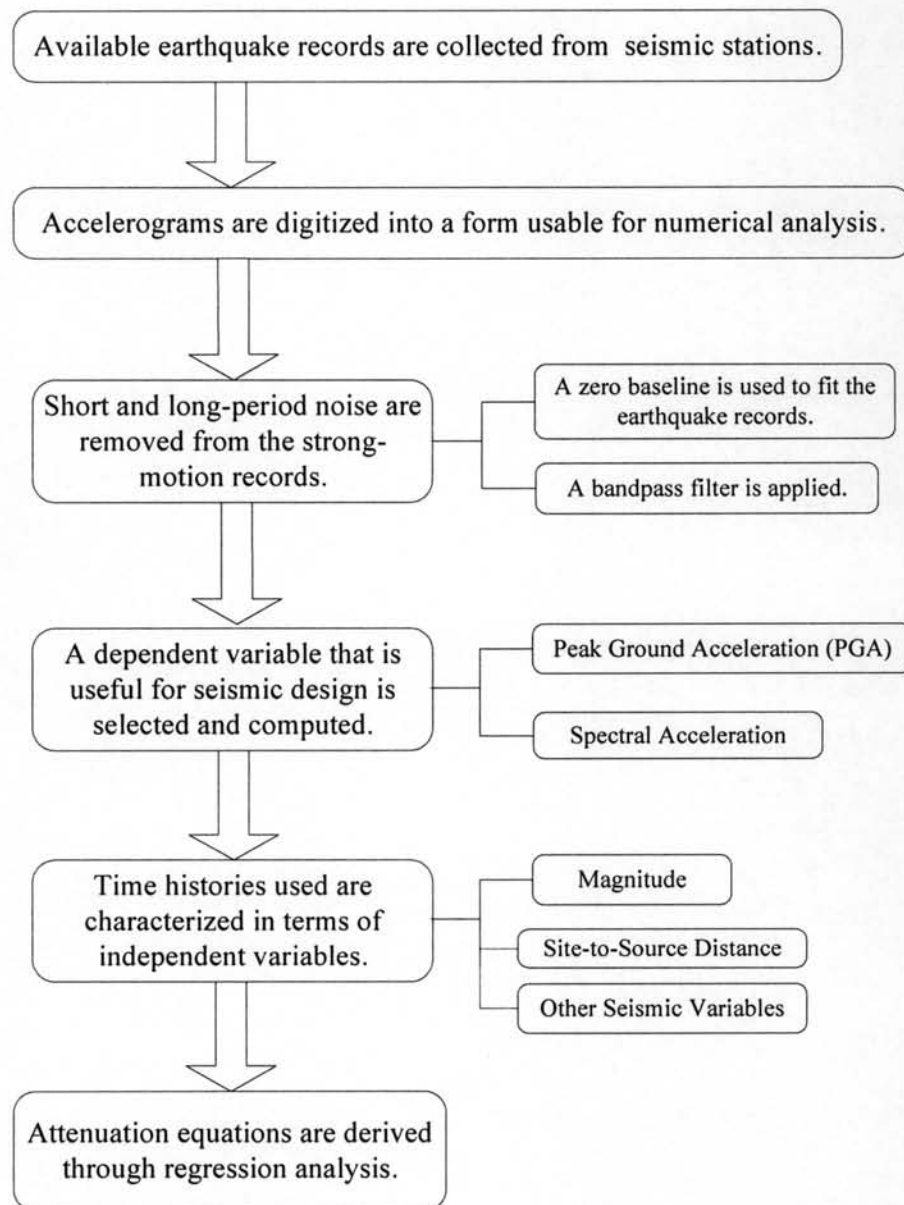
```
┌─────────────────────────────────────────────────────────────┐
│ Available earthquake records are collected from seismic      │
│ stations.                                                    │
└─────────────────────────────────────────────────────────────┘
                              │
                              ▼
┌─────────────────────────────────────────────────────────────┐
│ Accelerograms are digitized into a form usable for numerical │
│ analysis.                                                    │
└─────────────────────────────────────────────────────────────┘
                              │
                              ▼
┌──────────────────────────┐      ┌──────────────────────────┐
│ Short and long-period    │──────│ A zero baseline is used  │
│ noise are removed from   │      │ to fit the earthquake    │
│ the strong-motion        │      │ records.                 │
│ records.                 │      └──────────────────────────┘
│                          │      ┌──────────────────────────┐
│                          │      │ A bandpass filter is     │
│                          │      │ applied.                 │
└──────────────────────────┘      └──────────────────────────┘
                              │
                              ▼
┌──────────────────────────┐      ┌──────────────────────────┐
│ A dependent variable     │──────│ Peak Ground Acceleration │
│ that is useful for       │      │ (PGA)                    │
│ seismic design is        │      └──────────────────────────┘
│ selected and computed.   │      ┌──────────────────────────┐
│                          │      │ Spectral Acceleration    │
└──────────────────────────┘      └──────────────────────────┘
                              │
                              ▼
┌──────────────────────────┐      ┌──────────────────────────┐
│ Time histories used are  │──────│ Magnitude                │
│ characterized in terms   │      └──────────────────────────┘
│ of independent           │      ┌──────────────────────────┐
│ variables.               │      │ Site-to-Source Distance  │
│                          │      └──────────────────────────┘
│                          │      ┌──────────────────────────┐
│                          │      │ Other Seismic Variables  │
└──────────────────────────┘      └──────────────────────────┘
                              │
                              ▼
┌──────────────────────────┐
│ Attenuation equations    │
│ are derived through      │
│ regression analysis.     │
└──────────────────────────┘
```

Figure 3.1 General guidelines used in data processing to derive attenuation equations

Attenuation relations are employed once the earthquake distributions have

been calculated for all the faults to estimate the ground motion allocation for each earthquake of a particular magnitude, distance, and rupture mechanism. Moreover, these attenuation models allow the user to modify and update input parameters based on subjective input to obtain an assessment of seismic events (Petersen *et al.*, 1996).

To provide a best estimate of the standard error incurred in the regression, the deviation of the dependent variable from the fitted value is measured. This is termed as residual. It is an indicator of the aleatory or random variability of the dependent term. Based on previous studies, this standard deviation is represented as a function of magnitude and amplitude of ground motion. The trends of residuals are observed by plotting the residuals against seismic parameters such as magnitude or distance. The epistemic or modeling uncertainty can be recognized based on the visual inspection of these plots (Chen and Scawthorn, 2003).

3.2 Derivation of Attenuation Models

Various schemes and procedures concerning the formulation of attenuation relationships have been developed. To be able to derive a simple equation that is able to represent the ground motion in terms of predictor variables such as magnitude, distance and other descriptive seismic parameters, regression analysis of recorded ground motions is carried out in the process (Megawati *et al.*, 2005).

The coefficients in the equations are produced as a result of regression. Statistical fitting techniques such as least squares or maximum likelihood methods are used to process the ground motion data. This analysis is often conducted using any of the three procedures such as weighted nonlinear least-squares regression, two-step regression or random-effects method—all of which intends to alleviate the irregular distribution of the data set (Chen and Scawthorn, 2003).

Some of the methods by which researchers address the data sampling are as follows (Stewart *et al.*, 2001):

A two-step regression procedure is proposed by Joyner and Boore in 1981

wherein data points are weighted equally to come up with a shape of the function that depicts the spectral acceleration and distance relationship. Also, all events are weighted equally to quantify the dependence of spectral parameters with magnitude.

Campbell (1981) employed the weighted least squares technique by defining a bin of data corresponding to a limited range of magnitude and distance. In the regression, every bin of data is given equal weights. The data for each event within a bin are weighted equally too.

Random effects method is applied by Brillinger and Priesler in 1984 and 1985. The data set is corrected by considering the event-specific mean residuals which are referred to as event terms. The ground motion parameters are modified with respect to the difference of the event terms. From this corrected database, the regression coefficients are estimated. In this method, the likelihood of the event term due to random sampling of intra-event distribution as well as due to inter-event variability is evaluated.

Idriss developed a judgment based analysis in 1991 and 1994. The steps include postulation of model, analysis of residuals and modification of the model as deemed necessary.

In 2005, Megawati et al. derived attenuation relationships for Singapore and Malay Peninsula using synthetic seismograms. As part of simulation process, a reflectivity algorithm is employed wherein a seismic source is modeled as a dislocation point source having an approximate time function. Two functional forms of attenuation relationship were adopted for the prediction of horizontal and vertical components of ground motion. The adequacy of the model is checked through the available recorded data.

3.3   Factors Affecting Attenuation

3.3.1   Tectonic Setting

The tectonic regime where earthquakes happen affects ground motion properties. The three main tectonic categories include active tectonic regions,

subduction zones and stable continental regions. In active regions, indigenous attenuation relationships are derived empirically using strong motion data. For subduction zones that are situated at the interface between tectonic plates, database considered consists mostly of recordings at large distances. In stable continental regions, very few strong motion data are available. As a result, attenuation relationships are customarily based on simulated ground motions instead of recorded data (Stewart *et al.*, 2001).

3.3.2 Earthquake Magnitude

Magnitude represents the energy released during an earthquake. It is defined as the logarithm of certain peak ground motion parameter. The mathematical form of magnitude is expressed in equation 3.2.

$$M = \log_{10}(A) - \log_{10}(A_0) \qquad (3.2)$$

where

M	= magnitude;
A	= recorded trace amplitude of earthquake at a prescribed distance based on the recording instrument; and
A_0	= amplitude of a particular earthquake set as the standard.

Magnitude is based on the measurement of the maximum motion recorded by a seismograph. The most commonly used scales are designated as local magnitude M_L, surface wave magnitude M_s, body wave magnitude m_b, and moment magnitude M_W (Idriss and Archuleta, 2005).

3.3.3 Site-to-Source Distance

Numerous definition of site-to-source distance measures have been used by researchers in empirical attenuation models. This parameter illustrates the decay of ground motion as seismic waves propagate away from the source. Depending on the earthquake source as a single point or as a finite fault rupture, two groups of distance definition are available for use (Chen and Scawthorn, 2003).

Point source distance definition includes hypocentral (r_{hypo}) and

epicentral (r_{epi}) distances. r_{hypo} is measured from the site to a point in the Earth where rupture starts. r_{epi} is the distance measured from the site to the vertical projection of the hypocenter onto the Earth's surface.

For finite source distance measures, the commonly used distance definition includes r_{jb}, r_{rup} and r_{seis}. r_{jb} is the Joyner-Boore distance defined as the shortest horizontal distance to the vertical projection of the rupture plane. r_{rup} is the closest distance to the rupture plane. r_{seis} is the closest distance to the seismogenic part of the rupture plane (Chen and Scawthorn, 2003). Figure 3.2 further compares these distance definitions.

Vertical Faults

Dipping Faults
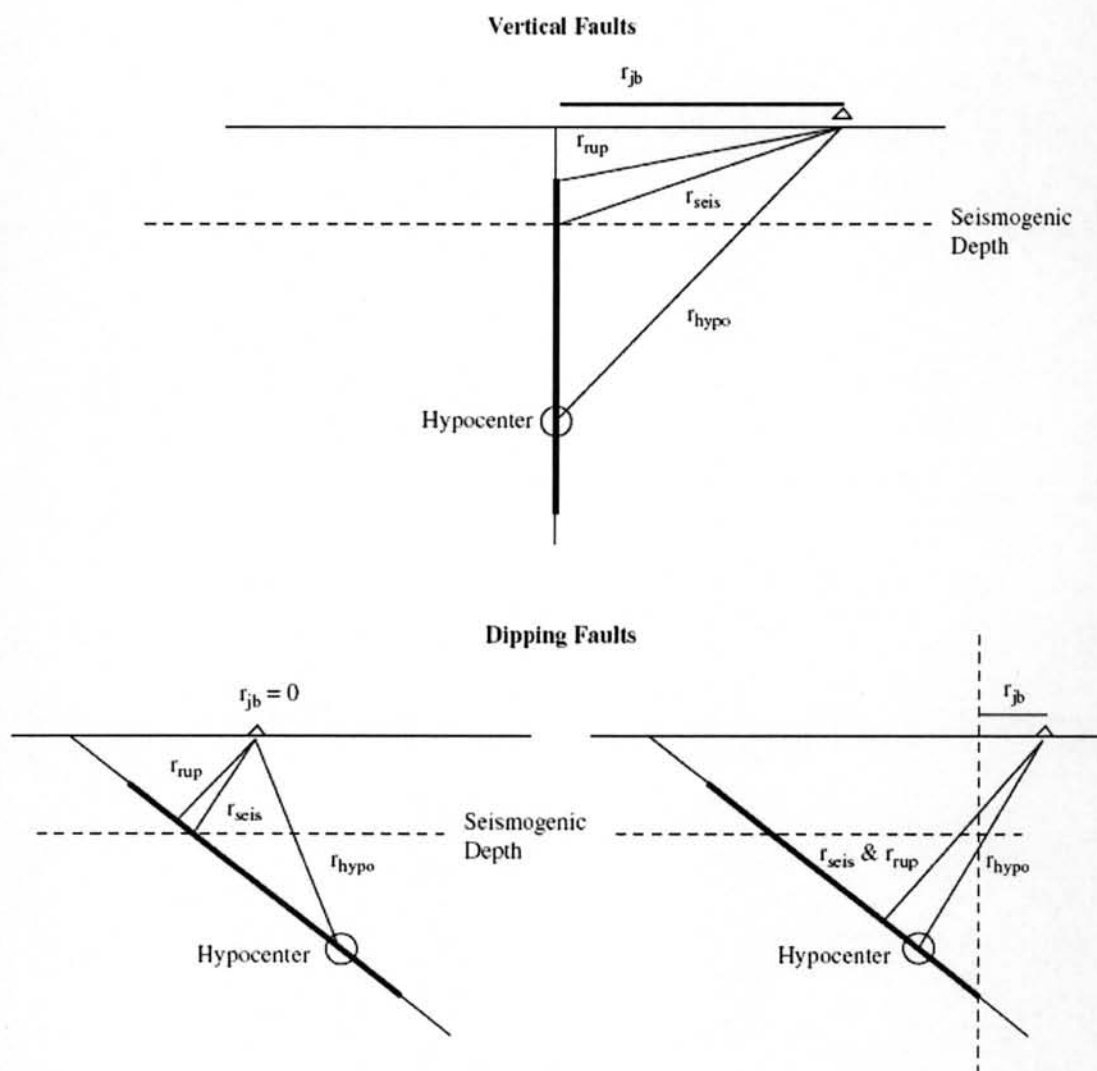
Figure 3.2 Comparison of distance definition (Abrahamson and Shedlock, 1997)

3.3.4 Local Site Conditions

Site factors take into account the geological and local properties of surface topography underlying the recording stations. To quantify the materials underneath the site up to the basement rock, shear wave velocity and the depth of sediments are analyzed (Chen and Scawthorn, 2003). Recent attenuation models use average shear wave velocity $\overline{V}_{s,30}$ in the upper 30 m of the Earth's surface to classify the site condition.

3.3.5 Faulting Mechanism

The seismological terms related to style of faulting factors include rake and strike. Rake is the angle between the directions of slip on the fault plane while strike represents the orientation of the fault. Based on these parameters, focal mechanism is categorized as strike slip, reverse slip and normal slip (Chen and Scawthorn, 2003).

3.3.6 Other Factors

The selection of factors is dependent on the researcher developing the model as there is no universal law to follow in formulating one. Other significant factors influencing the rate of attenuation may include stress drop, rupture process, hanging wall effects, dissipation of seismic energy as a result of earth's inelastic properties and focusing and scattering of elastic waves.

Stress drop quantifies the reduction in stress at fault surface following the rupture. This parameter influences the area of the ruptured surface and the fault slip displacement for a given seismic moment as the seismic waves propagate away from the source. High stress drop yields higher ground motions. Based on observations, Eastern North America (ENA) has higher stress drop average of about 200 bars compared with Western North America (WNA) which changes between 50 to 120 bars (Lam *et al.*, 2000).

Hanging wall is the part of the crustal regime that is situated on top of the rupture plane. Higher ground motions may be expected due to hanging-wall effect which is caused by the entrapment of seismic waves between the Earth's surface and

rupture plane (Chen and Scawthorn, 2003).

For path parameters, geometrical spreading describes the attenuation of amplitude of the propagating seismic waves due to geometrical spreading of energy. On the other hand, anelastic whole path attenuation deals with the energy loss as a result of the attenuation of shear wave amplitude when the number of wave cycles increases. Further to this, quality factor Q characterizes the wave transmission quality associated with the geology of a region under consideration. It is related to the regional mechanism that represents the frequency dependent attenuation properties. It quantifies the crustal energy absorption properties and rate of attenuation by taking into account the effects of whole path attenuation of seismic waves. In general, Q values are higher for older (harder) rocks in stable continental regions than younger (softer) rocks in mountainous regions (Lam *et al.*, 2000).

In the foregoing discussion, Q factor is represented by this expression:

$$Q=Q_0 \left(\frac{f}{f_o} \right)^n \tag{3.3}$$

where Q_0 and n are factors determined through local seismic monitoring of microtremors and aftershocks and f_o is a reference frequency equals to 1 Hz (Chandler and Lam, 2004).

Mid-crust modification factor allows adjustments for other parameters like density ρ of rock at the depth of rupture and shear wave velocity β. The upper crustal attenuation factor κ represents the attenuation of waves in the upper 4 km of the earth's crust. If the site is covered by sedimentary rocks, this parameter can be of great importance. The wave transmission quality of rocks near the earth's surface characterizes the upper crust attenuation. In stable continental regions like ENA, this factor is usually very high. Further to this, a list of values pertaining to the representative geological parameters that identify the wave path modification factors suitable for ENA and WNA crustal models is provided. These are listed in Table 3.1 (Lam *et al.*, 2000).

Table 3.1 Geological parameters of the generic crustal models

Parameter	Crustal Models	
	Hard Rock (ENA)	Rock (WNA)
Q_0	680	204
n	0.36	0.56
κ	0	0.0106M-0.012
β (m/s)	3,800	3,500
ρ (kg/m^3)	2,800	2,700
Mid-crust amplification factor	1.0	1.3

3.4   Next Generation Attenuation (NGA) Models

A research program directed by Pacific Earthquake Engineering Research Center – Lifelines Program (PEER-LL), U.S. Geological Survey (USGS) and Southern California Earthquake Center (SCEC) which started in 2002 aims to provide a new suite of Next Generation Attenuation (NGA) models. The program involves five developer teams that formulate new attenuation relationships independently under an interactive research project including Abrahamson and Silva, Boore and Atkinson, Campbell and Bozorgnia, Chiou and Youngs and Idriss. Each team utilizes their own set of data which is a subset of a common database compiled and processed by the same working group (Chiou *et al.*, 2006).

The main objective of the program is to merge views of experienced attenuation model developers and derive updated ground motion relationships for shallow crustal earthquakes in western U.S. In the process, an extensive review of source, path and site conditions is being conducted in an attempt to characterize strong ground motion records comprehensively. The database includes 173 events with 3,551 corrected and processed records measured on free-field conditions of recent large earthquakes. These records are described using 6 types of distance definition, 4 site classification schemes, shear wave velocity in every recording station, hanging wall and foot wall parameters and directivity measures (Chiou *et al.*, 2006).

These newly formulated attenuation relations are applicable to ground motion parameters of peak ground acceleration and velocity and spectral accelerations in the

period range of 0 (for PGA) to 10 seconds. Also, these equations are fit for use at M_w ranging from 5 to 8.5 within a distance range of 0 to 200 km (Chiou *et al.*, 2006).

In addition, NGA teams address the technical issues relating to magnitude scaling at close-in distances, directivity effects, style of faulting, polarization of near-field motion, non-linear amplification of shallow soil and sedimentary basin amplification. A well updated database of recorded ground motions is made available online in PEER NGA website (Chiou *et al.*, 2006).

3.5   Selection of Candidate Attenuation Models for Thailand

As mentioned previously, the development of attenuation relationship entails well-documented account of historical earthquake events that best represents the conditions of the site. But in the process, comprehensive understanding of the seismicity of a region is hampered by the scarcity in ground motion information. Major earthquake events are clustered in some areas. Traditional way of dealing with these conditions is to consider strong motion accelerograms from analogous regions with similar geological and seismo-tectonic features. However, this step has significant repercussions leading to misrepresentation of local conditions. As an end result, the analysis may generate empirical attenuation model that is not suitable for the study area (Lam *et al.*, 2005).

In connection to this, Shrestha cited in his study in 1987 that it is not possible to modify the existing attenuation relations or to formulate a new model specific for Thailand since the account of strong ground motion records is not sufficient enough to conduct the analysis.

Thus, in this study, the approach which is used to select the most suitable attenuation model for Thailand is by subjecting a number of existing attenuation models to further analysis. Eighteen attenuation relations are chosen to embody the propagation characteristics of earthquake events of the major tectonic settings. The selection is restricted to models that predict peak ground acceleration only as dictated by the availability of ground motion records in the country. These models are presumed to possibly provide essential information of Thailand's seismicity as

suggested in previous researches.

The succeeding section describes each of the selected models in detail.

3.5.1 Abrahamson and Silva (1997)

The attenuation equation of Abrahamson and Silva (1997) is represented by Equation 3.4.

$$\ln Y = f_1(M_w, r_{rup}) + f_2(M_w)F + f_3(M_w, r_{rup})HW + f_4(S, A_{rock}) \tag{3.4}$$

$$f_1(M_w, r_{rup}) = \begin{cases} 1.64 + 0.512(M_w - 6.4) + [-1.145 + 0.17(M_w - 6.4)]\ln R & \text{for } M_w \leq 6.4 \\ 1.64 - 0.144(M_w - 6.4) + [-1.145 + 0.17(M_w - 6.4)]\ln R & \text{for } M_w > 6.4 \end{cases}$$

$$f_2(M_w)F = \begin{cases} 0.610 & \text{for } M_w \leq 5.8 \\ 0.610 - \dfrac{0.35(M_w - 5.8)}{0.6} & \text{for } 5.8 < M_w < 6.4 \\ 0.260 & \text{for } M_w \geq 6.4 \end{cases}$$

$f_3(M_w, r_{rup})HW = f_{HW}(M_W)f_{HW}(r_{rup})$

$$f_{HW}(M_w) = \begin{cases} 0 & \text{for } M_w \leq 5.5 \\ M_w - 5.5 & \text{for } 5.5 < M_w < 6.5 \\ 1 & \text{for } M_w \geq 6.5 \end{cases}$$

$$f_{HW}(r_{rup}) = \begin{cases} 0 & \text{for } r_{rup} \leq 4\text{km} \\ 0.370[(r_{rup} - 4)/4] & \text{for } 4 < r_{rup} \leq 8\text{km} \\ 0.370 & \text{for } 8 < r_{rup} \leq 18\text{km} \\ 0.370[1 - ((r_{rup} - 18)/7)] & \text{for } 18 < r_{rup} \leq 25\text{km} \\ 0 & \text{for } r_{rup} > 25\text{km} \end{cases}$$

$f_4(S, A_{rock}) = [-0.417 - 0.230\ln(A_{rock} + 0.03)]S$

where

Y	= average horizontal or vertical component of PGA in g;
M_w	= moment magnitude;
r_{rup}	= closest distance to the rupture plane in km where $R = \sqrt{r_{rup}^2 + 5.60^2}$;
F	= type of faulting mechanism equal to 1 for reverse, 0.5 for reverse or

oblique and 0 otherwise;

HW = hanging wall effect equal to 1 for sites located on hanging wall and 0 otherwise;

S = site category equal to 0 for rock site and 1 for soil site; and

A_{rock} = average peak acceleration on rock as predicted by the model when S=0.

This equation is applicable for shallow crustal earthquakes of active tectonic regime. It is derived using 655 recordings from 58 worldwide earthquake events. The relation takes into account the significant increase in ground motions for the sites located over the hanging wall as compared with the sites located on a foot wall. This model is considered valid for M_w equals 4.4 to 7.4 and r_{rup} from 0 to 220 km (Abrahamson and Silva, 1997).

It was noted that the data set created for this model is biased towards larger motions. The reason is that different bandwidths are used depending on each recording rather than employing a single usable bandwidth for all data. Data set consists of larger than average ground motions since the former has greater chances of being above the noise level.

The total standard error σ_{total} of the model is a sum of intra-event and inter-event errors. It is magnitude dependent as indicated in equation 3.5 (Abrahamson and Silva, 1997).

$$\sigma_{total}(M) = \begin{cases} 0.70 & \text{for } M \leq 5.0 \\ 0.565(M-5) & \text{for } 5.0 < M < 7.0 \\ 0.430 & \text{for } M \geq 7.0 \end{cases} \tag{3.5}$$

3.5.2 Ambraseys *et al.* (2005)

The functional form proposed by Ambraseys *et al.* (2005) for PGA is as follows:

$$\log Y = 2.522 - 0.142M_w + (-3.184 + 0.314M_w)\log\sqrt{r_{jb}^2 + 7.6^2} + 0.137S_S + 0.05S_A - 0.084F_N$$

$$+ 0.062F_T - 0.044F_O \tag{3.6}$$

where

Y = horizontal PGA in m/s^2;

M_w = moment magnitude;

r_{jb} = distance to the surface projection of the fault;

S_S = 1 for very soft and soft soil sites and 0 otherwise;

S_A = 1 for stiff soil sites and 0 otherwise;

F_N = 1 for normal faulting earthquakes and 0 otherwise;

F_T = 1 for thrust faulting earthquakes and 0 otherwise; and

F_O = 1 for odd faulting earthquakes and 0 otherwise.

Weighted regression analysis is used in a set of 595 strong motion records in Europe and Middle East. The data set consists of records with magnitude range of 5.0 to 7.6 and distance range of 0 to 100 km. This model considers four site categories based on the range of shear wave velocity $\overline{V}_{S,30}$, the descriptions of which are tabulated below in Table 3.2. Effect of faulting mechanism to the observed ground motions is also incorporated in the equation.

Table 3.2 Ambraseys *et al.* (2005) definition of site category

Site Category	$\overline{V}_{S,30}$ (m/s)
Very soft soil	$\overline{V}_{S,30} \leq 180$ m/s
Soft soil	$180 < \overline{V}_{S,30} \leq 360$ m/s
Stiff soil	$360 < \overline{V}_{S,30} \leq 750$ m/s
Rock	$\overline{V}_{S,30} > 750$ m/s

The associated errors of the proposed model representing intra and inter-earthquake standard deviations respectively are as follows (Ambraseys *et al.*, 2005).

$$\sigma_{intra} = 0.665\text{-}0.065M_w \qquad (3.7a)$$

$$\sigma_{inter} = 0.222\text{-}0.022M_w \qquad (3.7b)$$

3.5.3 Boore, Joyner and Fumal (1997)

The attenuation model of Boore *et al.* (1997) is expressed in Equation 3.8.

$$\ln Y = -0.242 + 0.527(M_w - 6) - 0.778\ln r - 0.371\ln\left(\frac{V_s}{1396}\right) \qquad (3.8)$$

where

Y = geometric mean of two horizontal components of acceleration in g;

M_w = moment magnitude;

r = $\sqrt{r_{jb}^2 + h^2}$ where r_{jb} is the Joyner-Boore distance which is the closest horizontal distance from the station to a point on the Earth's surface that lies directly above the rupture and h is equals to 5.57 which is a fictitious depth determined from the regression; and

V_S = average shear wave velocity over the upper 30 m of the profile under consideration in m/s.

The attenuation relation considers site conditions for strike-slip, reverse slip and unspecified faulting mechanisms. But since in this research, there is no available data for types of faulting, the coefficient representing the earthquakes without specified mechanism is utilized.

Weighted, two-stage method is used as regression technique. The attenuation relation is intended to be used for magnitude ranging from 5.5 to 7.5 at distances not greater than 80 km. The standard deviation σ of the data about the prediction equation for peak horizontal acceleration is equals to 0.520 (Boore *et al.*, 1997).

3.5.4 Campbell (1997)

The ground motion attenuation relationship of Campbell (1997) is

$$\ln Y = -3.512 + 0.904M_w - 1.328\ln\sqrt{r_{seis}^2 + [0.149\exp(0.647M_w)]^2} + [1.125 - 0.112\ln(r_{seis})$$

$$-0.0957M_w]F + [0.440 - 0.171\ln(r_{seis})]S_{SR} + [0.405 - 0.222\ln(r_{seis})]S_{HR} \qquad (3.9)$$

where

Y	= geometric mean of two horizontal components of PGA in g;
M_w	= moment magnitude;
r_{seis}	= closest distance from the recording site to the seismogenic rupture in km;
F	= style of faulting where F = 0 for strike-slip faulting and F = 1 for reverse, thrust, oblique and thrust-oblique faulting; and
S_{SR} and S_{HR}	= local site conditions

where

S_{SR} = S_{HR} = for alluvium or firm soil = 0;

S_{SR} = 1 and S_{HR} = 0 for soft rock; and

S_{SR} = 0 and S_{HR} = 1 for hard rock.

The equation is developed using near-source recordings to reduce the effect of regional differences in crustal attenuation and to prevent the influence of complex propagation due to long distances. The ground motion database consists of magnitude ranging from 4.7 to 8 at distance range of 3 to 60 km. To determine the coefficients, an unweighted generalized nonlinear least-square regression is used.

To account for the component of variability in the model, the standard error of ln Y, σ, is expressed as a function of earthquake magnitude as well as of ln Y. The resulting relationship between σ and ln Y is given in equation 3.10.

$$
\begin{aligned}
\sigma &= 0.55 &&\text{when } Y < 0.068g; \\
\sigma &= 0.173 - 0.140\ln(Y) &&\text{when } 0.068g \leq Y \leq 0.21g; \\
\sigma &= 0.39 &&\text{when } Y > 0.21g
\end{aligned}
\tag{3.10}
$$

The relationship that relates σ and M is given by

$$
\begin{aligned}
\sigma &= 0.889 - 0.0691M &&\text{when } M < 7.4; \\
\sigma &= 0.38 &&\text{when } M \geq 7.4
\end{aligned}
\tag{3.11}
$$

3.5.5 Esteva and Villaverde (1973)

The functional form of this model is

$$Y = \frac{1230\exp^{0.8M}}{(R+25)^2}$$ (3.12)

where

Y   = PGA in cm/s²;

M   = magnitude; and

R   = hypocentral distance in km.

The range of magnitude of the data set used in this model is not defined but for distance values, it is applicable within the range of 15 to 150 km. The standard deviation of the natural logarithm of observed to computed intensities is equals to 1.02. This equation has been included in various researches as a candidate model suitable for Thailand as mentioned in the literature review. Although this attenuation relation is not well-updated in terms of database used, it is still included in this study to assess its reliability in handling earthquake ground motions that could possibly affect Thailand.

3.5.6 Idriss (1993)

A good number of horizontal recordings in rock sites from 30 earthquake events are used to derive this attenuation model. The equation is divided into M < 6.0 and M ≥ 6.0 using local M_L and surface wave magnitude M_S scales respectively. The range of applicability is 1 to 100 km for distance and 4.6 to 7.4 for magnitude (Douglas, 2004).

The equation is as follows:

$$\ln Y = [C_1 + \exp(C_2 + C_3 M)] - [\exp(C_4 + C_5 M)]\ln(r_{rup} + 20) + 0.2F$$ (3.13)

where

Y   = horizontal PGA in g;

M   = local magnitude for M<6 and surface wave magnitude M≥6;

r_{rup} = shortest distance to the rupture plane in km;

F   = fault mechanism such that F=0 for strike slip, 0.5 for oblique and 1
for reverse;

$C_1 = -0.150$, $C_2 = 2.261$, $C_3 = -0.083$, $C_4 = 1.602$ and $C_5 = -0.142$ for $M \le 6.0$;

$C_1 = -0.050$, $C_2 = 3.477$, $C_3 = -0.284$, $C_4 = 2.475$ and $C_5 = -0.286$ for $M > 6.0$;

$\sigma = 1.39 - 0.14M$ for $M < 7\frac{1}{4}$; and

$\sigma = 0.38$ for $M \ge 7\frac{1}{4}$.

3.5.7 Sabetta and Pugliese (1987)

This model is represented by

$$\log_{10} Y = -1.562 + 0.306M - \log_{10}\sqrt{r^2 + 5.8^2} + 0.169S \tag{3.14}$$

where

Y	= larger horizontal component of PGA in g;
M	= M_S for $M \ge 5.5$ and M_L otherwise;
r	= distance to surface projection of fault in km;
S	= site category such that S=0 for stiff and deep soil with Vs>800 m/s and depth of soil H>20m and S=1 for shallow soil at soil depth ranging from 5 to 20m; and
σ	= 0.173.

The data used in the derivation of the equation is limited to the available records in Italy. 95 records from 17 earthquakes with magnitudes between 4.6 to 6.8 at a distance range of 1.5 to 180 km comprise the data set. A combination of magnitude scales is used wherein 5.5 is the change-over point used to change from M_L to M_S. It was noted that the model may be restricted by the small suite of records such that beyond the range prescribed, the estimated ground motions may be incorrect (Douglas, 2003).

3.5.8 Sadigh et al. (1997)

This attenuation model can be used to estimate ground motions for rock sites. Rock site is defined as the site with bedrock in about one meter from the surface. Along with this model, a relationship suitable for spectral acceleration for deep soil sites is also derived using normalized PGA recordings. Strong motion recordings from California earthquakes are the primary data used with earthquakes of M_w ranging from 4 to 8 and distances up to 100 km (Sadigh et al., 1997).

Attenuation equation is given as follows:

$$\ln Y = C_1 + C_2 M_w + C_3 \ln(r_{rup} + \exp(C_4 + C_5 M_w)) + C_6 Z_T \qquad (3.15)$$

where

Y = geometric mean of horizontal components of PGA in g;

M_w = moment magnitude;

r_{rup} = minimum distance to the rupture surface in km;

Z_T = dummy variable equals to 1 for reverse-faulting earthquakes and 0 for strike-slip;

$C_1 = -0.624$, $C_2 = 1.0$, $C_3 = -2.1$, $C_4 = 1.29649$ and $C_5 = 0.250$ for $M \leq 6.5$; and

$C_1 = -1.274$, $C_2 = 1.1$, $C_3 = -2.1$, $C_4 = -0.48451$ and $C_5 = 0.524$ for $M > 6.5$.

The standard errors are found to be magnitude dependent such that for horizontal PGA at rock sites at $M<7.21$, $\sigma = 1.39 - 0.14M$ and at $M \geq 7.21$, $\sigma = 0.38$.

3.5.9 Spudich *et al.* (1997)

The attenuation relation is

$$\log_{10} Y = 0.156 + 0.229(M_w - 6) - 0.945 \log_{10} R + 0.077S \qquad (3.16)$$

where

Y = peak horizontal acceleration in g;

M_w = moment magnitude;

R $= \sqrt{r_{jb}^2 + 5.57^2}$ where r_{jb} is the Joyner-Boore distance in km which is the shortest distance from the station to the vertical projection on the Earth's surface of the rupture area;

S = 0 for rock sites and 1 for soil sites; and

$\sigma_{\log Y}$ = 0.310.

This predictive relation is derived based on the database from worldwide extensional environments. Extensional tectonic regimes are defined as those where the crust is lengthening or being pulled apart. Such environment typically exists in the Basin and Range province of Eastern California as well as in Western Europe like parts of Italy and Greece. As specified in the original publication, SEA96 is suitable in the 5.0-7.7 magnitude range and 0-70 km distance range (Spudich *et al.*,

1997).

3.5.10 Atkinson and Boore (1997b)

The model is represented by

$$\ln Y = 1.841 + 0.686(M_w - 6) - 0.123(M_w - 6)^2 - \ln r_{hypo} - 0.00311 r_{hypo} \tag{3.17}$$

where

Y = average horizontal component of PGA in g;

M_w = moment magnitude; and

r_{hypo} = hypocentral distance = $\sqrt{R_o^2 + h^2}$ where R_o is the closest distance from the site to the projection of the fault and h is the focal depth in km.

The relation is considered to be valid for M_w ranging from 4 to 7.5 at distances starting from 10 to 500 km. Ground motion estimates apply to bedrock sites which correspond to Eastern North America (ENA) deep stiff soil setting with soil depth greater than 60 meters and $\overline{V}_{S,30}$ in the order of 500 m/s (Atkinson and Boore, 1997).

3.5.11 Dahle *et al.* (1995)

Dahle *et al.* have used other magnitude scales, for instance M_s, body wave magnitude m_b and duration magnitude M_D for events without estimates of M_w. Bayesian one-stage method is the regression technique utilized to arrive at logical sets of coefficients. Earthquake records from Costa Rica, Nicaragua and El Salvador comprise the database and the validity of the model is within a magnitude range of 3 to 8 and distance range from 6 to 490 km. The larger of the two horizontal components of PGA is used with a total of 280 records from 72 earthquakes (Douglas, 2004).

The model is defined by Equation 3.18.

$$\ln Y = -1.579 + 0.554 M_w - 0.560 \ln\sqrt{r_{hypo}^2 + 6^2} - 0.0032\sqrt{r_{hypo}^2 + 6^2} + 0.326 S \tag{3.18}$$

where

Y = horizontal component of PGA in m/s^2;

M_w = moment magnitude;

r_{hypo} = hypocentral distance;

S   = site category equal to 1 for soil sites and 0 for rock sites; and

σ = 0.3535.

3.5.12 Hwang and Huo (1997)

The model is represented by the following equation:

$$\ln Y=-2.904+0.926M_w-1.271\ln[\sqrt{r_{epi}^2+H^2}+0.06\exp(0.7M_w)]-0.0032\sqrt{r_{epi}^2+H^2} \quad (3.19)$$

where

Y   = PGA at the bedrock sites in unit of g;

M_w = moment magnitude;

r_{epi} = epicentral distance;

H   = focal depth which is usually taken as 10 km in Central and Eastern United States;

$\sigma_{\ln Y}$ = variability of ground motion parameter equals to 0.309.

This attenuation model is fit to use in estimating earthquake ground motions for epicentral distances with a lower bound of 5 km and an upper bound of 200 km at magnitude range of 5.0 to 7.5. Bedrock sites are described as having $\overline{V_{s,30}}$ of about 3.5 km/s (Hwang and Huo, 1997).

3.5.13 Toro (2002)

Toro (2002) is a modified version of the model derived by Toro, Abrahamson and Schneider in 1997. In this equation, R_M is adjusted in order to fit the database from California characterized as having large magnitudes at short distances. This latest model accounts for the magnitude saturation and the variations in source scaling. Gulf Coast and Mid-continent crustal regions are considered separately by specifying different sets of regression coefficients. The relation is formulated using stochastic method for M_w from 5.0 to 8.0 at r_{jb} from 1 to 500 km (Toro, 2002).

$$\ln Y=C_1+C_2(M_w-6)-C_3\ln R_M-(C_4-C_3)f(R_M)-C_5R_M \quad (3.20)$$

where

Y   = PGA in g;

M   = moment magnitude;

R_M = $\sqrt{r_{jb}^2 + C_6^2[\exp(-1.25 + 0.227M)]^2}$ where r_{jb} is Joyner-Boore distance in km;

$f(R_M)$ = 0 for $r_{jb} \leq 100$ km and $f(R_M) = \ln(r_{jb}/100)$ for $r_{jb} > 100$ km;

$C_1 = 2.91$, $C_2 = 0.92$, $C_3 = 1.49$, $C_4 = 1.61$, $C_5 = 0.0014$ and $C_6 = 10.9$ for Gulf region;

$C_1 = 2.20$, $C_2 = 0.81$, $C_3 = 1.27$, $C_4 = 1.16$, $C_5 = 0.0021$ and $C_6 = 9.3$ for Mid-continent regions.

3.5.14 Atkinson and Boore (1997a)

The relation is specifically derived for Cascadia subduction region for rock sites through the simulation of recordings at magnitude range of 4 to 8.25 and hypocentral distances from 10 to 400 km. However, the database does not contain data points at magnitude range of 6.8 to 7.4. A good number of events within the magnitude range of 4 to 5.5 represent the Cascadia data while large magnitude events are taken from other subduction zones (Atkinson and Boore, 1997).

$$\ln Y = 0.680 + 0.733(M_w - 6) - \ln r_{hypo} - 0.006451 r_{hypo} \tag{3.21}$$

where

Y   = average horizontal component of PGA in g;

M_w = moment magnitude; and

r_{hypo} = hypocentral distance = $\sqrt{R_o^2 + h^2}$ where R_o is the closest distance from the site to the projection of the fault and h is the focal depth in km.

3.5.15 Crouse (1991)

This model considers worldwide subduction environment as area of interest. The regression equation developed estimates PGA at shallow firm soil sites in the Pacific Northwest. Data recorded at stiff soil sites are more prominent than rock data. Also, database includes accelerograms recorded from the basement of buildings.

Other scales of magnitudes are considered such as M_S and Japanese Meteorological Agency magnitude M_{JMA} to arrive at a good estimate of M_w. Database consists of recordings with magnitude equals to 4.8 to 8.2, focal depth ranging from 0 to 238 km and distances from 8 to 850 km. Ground motion estimated by this relation is for generic soil sites with V_{s30} equivalent to 310 m/sec (Crouse, 1991).

$$\ln Y = 6.36 + 1.76 M_w - 2.73 \ln[R + 1.58 \exp(0.608 M_w)] + 0.00916h \qquad (3.22)$$

where

Y	= average horizontal component of PGA in cm/s^2;
M_w	= moment magnitude;
R	= distance to the center of the energy release on the fault;
h	= focal depth in km; and
σ	= standard error of ln(PGA) equal to 0.773.

3.5.16 Megawati *et al.* (2005)

$$\ln Y = -7.198 + 2.3691 M_w - 0.013856 M_w{}^2 - \ln r - 0.001548r - 0.08909h \qquad (3.23)$$

where

Y	= horizontal PGA in cm/s^2;
M_w	= moment magnitude;
r	= source-to-site distance in km;
h	= focal depth in km; and
σ	= standard deviation of the residuals equal to 0.4413.

Using the fundamental concepts of wave propagation in elastic media, Megawati *et al.* formulated the attenuation model for rock sites to address the need to approximate ground motions caused by distant earthquakes defined as events with R more than 300 km. Specifically, this model assesses the ground motion in Singapore and Kuala Lumpur due to the great Sumatran subduction earthquake. The model covers a distance range of 198 to 1422 km with M_w ranging from 4.5 to 8.0.

3.5.17 Petersen *et al.* (2004)

To quantify the hazard across the southern Malaysian Peninsula and Sumatra, Indonesia, Petersen *et al.* conducted a seismic hazard analysis in 2004. As a

result, a modification of the Youngs *et al.* attenuation model in 1997 is proposed to account for peak ground acceleration at distances beyond 200 km.

$$\ln Y = 0.2418 + 1.414M_w - 2.552\ln(r_{rup} + 1.7818e^{0.554M_w}) + 0.00607H + 0.3846Z_T$$

$$-0.0038(r_{rup} - 200) \tag{3.24a}$$

$$\ln Y = -0.6687 + 1.438M_w - 2.329\ln(r_{rup} + 1.097e^{0.617M_w}) + 0.00648H + 0.3643Z_T$$

$$-0.0038(r_{rup} - 200) \tag{3.24b}$$

where

Y	=	geometric mean of two horizontal components of PGA in g;
M_w	=	moment magnitude;
r_{rup}	=	closest distance to rupture in km;
H	=	focal depth in km;
Z_t	=	source type such that 0 for interface and 1 for intraslab; and
σ	=	1.45-0.1M which is applicable for both rock and soil sites.

(σ for magnitudes greater than 8 is set equal to the value for M=8).

In this study, the modified version is named after the original authors of the equation with the year when it was modified. Equation 3.24a listed above is for rock sites while the succeeding equation represents soil sites. The attenuation models represent the interface and intraslab earthquakes in subduction zones of moment magnitude 5 to 8.2 and for distance from 10 to 500 km. Interface earthquakes include events that happen along the boundary of subducting and intervening plates which are usually of low-angle thrust faulting type. In contrast, intraslab earthquakes are high-angle normal faulting events that transpire inside the subducting plate (Youngs *et al.*, 1997).

3.5.18 Fukushima and Tanaka (1991)

The attenuation model given in eq. 3.25 is intended to estimate ground motions in Japan for near earthquake sources. Database is composed of 1,372 horizontal components of PGA from 28 earthquakes in Japan and 15 earthquakes in United States and other countries. The magnitude ranges from 4.5 to 8.2 at a distance range of 10 to 300 km. The model yields ground motion at the surface, thus,

correction is necessary in order to predict the peak acceleration at the bedrock. The average peak horizontal accelerations for rock and soil sites are 60 and 140 percent correspondingly of the predicted PGA from the formula (Fukushima and Tanaka, 1991).

$$\log_{10}(Y)=0.41M_s-\log_{10}[R+(0.032\times10^{0.41M_s})]-0.0034R+1.30 \qquad (3.25)$$

where

     Y   = mean of the peak acceleration from two horizontal components in cm/s^2;

     M_S = surface wave magnitude; and

     R   = shortest distance between site and fault rupture in km.

Table 3.3 lists the selected attenuation models grouped according to tectonic regimes. In line with this, the range of magnitude and distance used in the development of each model is also summarized. However, it should be noted that various models have different definitions of magnitude and distance used in the regression analysis. Such variation is not indicated in the table.

In Table 3.4, models which take into account the focal mechanisms in the derivation of the equation are summarized. On the other hand, the main characteristics of the selected attenuation models are stipulated in Tables 3.5, 3.6 and 3.7 for crustal models of stable continental regions and active tectonic regions as well as for the subduction zone models respectively. These tables provide an overview of the predictor variables used in the equation with a level of detail deemed sufficient for the evaluation of the candidate attenuation models for Thailand.

Table 3.3 Selected attenuation models with suitable ranges of applicability

Attenuation Model	Model Notation	Distance Range (km)	Magnitude Range
Active Tectonic Regions			
Abrahamson and Silva (1997)	AS97	0-220	4.4-7.4
Ambraseys *et al.* (2005)	AB05	0-100	5.0-7.6
Boore *et al.* (1997)	BJF97	0-80	5.5-7.5
Campbell (1997)	CB97	3-60	4.7-8.0
Esteva and Villaverde (1973)	EV73	15-150	-
Idriss (1993)	ID93	1-100	4.6-7.4
Sabetta and Pugliese (1987)	SP87	1.5-180	4.6-6.8
Sadigh *et al.* (1997)	SD97	0-100	4.0-8.0
Spudich *et al.* (1997)	SEA97	0-70	5.0-7.7
Stable Continental Regions			
Atkinson and Boore (1997b)	AB97b	10-500	4.0-7.5
Dahle *et al.* (1995)	DH95	6-490	3.0-8.0
Hwang and Huo (1997)	HH97	5-200	5.0-7.5
Toro (2002)	TR02	1-500	5.0-8.0
Subduction Zones			
Atkinson and Boore (1997a)	AB97a	10-400	4.0-8.0
Crouse (1991)	CR91	8-850	4.8-8.2
Megawati *et al.* (2005)	MW05	198-1422	4.5-8.0
Petersen *et al.* (2004)	PT04	10-500	5.0-8.2
Fukushima and Tanaka (1991)	FT91	10-300	4.5-8.2

Table 3.4 List of attenuation models that consider source mechanism as predictor variable

Attenuation Model	Description of source mechanism
Abrahamson and Silva (1997)	F=1 for reverse, 0.5 for reverse/oblique and 0 for normal or strike-slip
Ambraseys *et al.* (2005)	F_N=1 for normal faulting earthquakes and 0 otherwise; F_T=1 for thrust faulting earthquakes and 0 otherwise; and F_O=1 for odd faulting earthquakes and 0 otherwise.
Boore *et al.* (1997)	B_{1SS} = -0.313 for strike-slip earthquakes; b_{1RS} =-0.117 for reverse-slip earthquakes; and b_{1ALL} =-0.242 if mechanism is not specified.
Campbell (1997)	F=0 for strike-slip faulting and 1 for reverse, thrust, oblique and thrust-oblique faulting.
Idriss (1993)	F=0 for strike-slip, 0.5 for oblique and 1 for reverse.
Sadigh *et al.* (1997)	Z_T=1 for reverse-faulting earthquakes and 0 for strike-slip.
Petersen *et al.* (2004)	Z_T=0 interface earthquakes of low angle, thrust faulting shocks occurring on plate interfaces and 1 for intraslab earthquakes of high angle, predominantly normal faulting shocks

Table 3.5 Main characteristics of selected attenuation models in active tectonic regions for median peak ground acceleration

Model Notation	Regression Method	Data Used [1]	Magnitude Scale [2]	Distance Definition [3]	Site Parameters	Other Parameters [4]
AS97	Random Effects	Mostly California earthquakes $\leq$58 E; H$\leq$655; V$\leq$650	M_w	r_{rup}	S_{rock}=0 and S_{soil}=1	HW, F, h
AB05	Weighted regression analysis	Europe; Middle East 595 records	M_w	r_{jb}	Very soft and soft soil sites; Stiff soil sites	F, h
BJF97	Two-stage regression	WNA 20E; H=271	M_w	r_{jb}	$V_{s,30}$	F, h
CB97	Ordinary one-stage	Worldwide 47E; H=645 26E; V=225	M_w	r_{seis}	Alluvium or firm soil; soft rock; hard rock	F
EV73	-	Western USA	-	r_{hypo}	-	-
ID93	-	30E; H=572	M_L for M<6; M_S for M$\geq$6	r_{rup}	Rock only	F
SP87	Ordinary one-stage	Italy 17E; H=95	M_S for M$\geq$5.5; M_L otherwise	r_{jb}	Stiff and deep soil; Shallow soil	h
SD97	-	Mostly California earthquakes 119E: H=960	M_w	r_{rup}	Rock only	F
SEA97	Maximum likelihood two-stage	Worldwide extensional regimes 30E; H=128	M_w	r_{jb}	Rock and soil	h

[1] E = number of earthquakes; H = horizontal records; V = vertical records;

[2] M_w = Moment magnitude; M_s = Surface-wave magnitude; M_L = Local magnitude; M_{JMA} = Japanese Meteorological Agency magnitude; M_D = Duration magnitude; m_b = Body wave magnitude;

[3] r = site-to-source distance; r_{hypo} = hypocentral distance; r_{cen} = center of energy release distance; r_{jb} = surface projection distance or Joyner and Boore distance; r_{rup} = distance to rupture plane; r_{seis} = closest distance to seismogenic part of the rupture plane; r_{epi} = epicentral distance

[4] HW = hanging wall effect; F = focal mechanism; h = focal depth; Z_t = subduction zone source factor

Table 3.6 Main characteristics of selected attenuation models in stable continental regions for median peak ground acceleration

Model Notation	Regression Method	Data Used	Magnitude Scale	Distance Definition	Site Parameters	Other Parameters
AB97b	Two-corner frequency	ENA	M_w	r_{hypo}	Rock only	h
DH95	Bayesian one-stage	Central America 72E; H=280	M_w if available; otherwise M_s, M_D or m_b	r_{hypo}	Rock and soil	h
HH97	Seismological Model	Central and Eastern US	M_w	r_{epi}	Rock only	h
TR02	One-corner frequency	CENA	M_w	r_{jb}	Rock only	-

Table 3.7 Main characteristics of selected attenuation models in subduction zones for median peak ground acceleration

Model Notation	Regression Method	Data Used	Magnitude Scale	Distance Definition	Site Parameters	Other Parameters
AB97a	Simulation	Cascadia regions	M_w	r_{hypo}	Rock only	h
CR91	Ordinary one-stage	Worldwide subduction zones	M_w if available; otherwise M_s or M_{JMA}	r_{cen}	Firm soil only	h
MW05	Reflectivity Theorem	42 Sumatran earthquakes	M_w	r	Rock only	h
PT04	-	Worldwide subduction zones	M_w	r_{rup}	Rock and soil	Z_t, h
FT91	Multiple regression analysis	Mostly from Japan; others from US 28E; H=1,372	M_S	r_{rup}	Rock and soil	-

3.6   Comparison of Selected Attenuation Models to Data Set 1

The comparison of attenuation curves of PGA has been performed for moment magnitudes ranging from 4.0 to 9.0. The geometric mean of the two horizontal components of PGA is computed using the actual field records measured from TMD's

old digital seismic stations. In this study, this variable that is being predicted by the attenuation models is defined in this manner since most of the selected candidate models use this definition as well as most of the NGA models.

The ground motion records are then calibrated in each model in accordance with site categories and earthquake epicenters whether of crustal or subduction type. Figures 3.3 to 3.5 show the attenuation curves generated for the models in rock sites while Figures 3.6 to 3.7 depict the attenuation curves in soil sites.

Consistent with the definition of attenuation, all curves depict the decrease in the intensity of ground motion with increasing distance and decreasing magnitude. A basic observation for all the plots generated is that the actual acceleration ground motions recorded by TMD's digital stations are lower compared with the estimated acceleration values of most attenuation models.

The generation of curves for specific magnitude is dictated by the availability of actual data in each category under consideration. For non-subduction zone models involving active tectonic regions and stable continental regions, the recordings have magnitude values ranging from 3.8 to 5.8. Thus, three attenuation curves for each of these models are plotted at magnitudes 4, 5 and 6. The field records are grouped using a bin of 1 magnitude, ranging from half a magnitude lower to half a magnitude higher than the reference magnitude. It could also be observed from the graphs that a lot of data points are considered in subduction zone models since 90% of the events in the database are of subduction type. It is for this reason that a number of attenuation relations representing the subduction zones have been included in the analysis although most earthquakes within approximately 600 km radius from Bangkok belong to shallow crustal type as mentioned by Warnitchai *et al.* (2000).

For attenuation curves of PGA in rock sites, several models in active tectonic regions (Figure 3.3), e.g., ID93, SD97, EV73 and CB97, and stable continental regions (Figure 3.4), e.g., TR02Gulf and HH97, correlate well with the low-rate attenuation characteristic of Thailand. Some of the equations, however, such as SP87, BJF97 and SEA97, over-predict the PGA at large distances. Some subduction zone models (Figure 3.5), e.g., MW05 and CR91, seem to correspond to field records quite

well compared with other models in the same tectonic regime although MW05 overestimates the ground motion at large magnitude.

For attenuation curves of PGA in soil sites (Figure 3.6), AB05, AS97 and CB97 fit the data points reasonably well for non-subduction zone models. Only the model proposed by DH95 has catered for soil site parameter among the models in stable continental regions. Conversely, two subduction models have soil site parameters (Figure 3.7) such as PT04 and FT91. PT04 fit the recordings better compared with FT91 based on Figure 3.7.

It is prevalent in all of the plots that some points deviate from the predicted PGA values such that there is no model that perfectly fits the actual records. By observing these graphical representations of attenuation models, a trend that is common in every tectonic setting can be recognized.

In active tectonic regions, models of AS97, AB05, and ID93 generate attenuation curves for different magnitudes that diverge at long distances. This is because the rate of attenuation in these models is dependent on magnitude, i.e., slower rate at higher magnitudes, whereas the rate of attenuation for other models belonging to this tectonic region is essentially independent of magnitude.

Curves of low attenuation rate are reflected in models of stable continental regions as depicted in Figure 3.4. The range of applicability of these models is usually up to a distance of 500 km. Beyond 500 km, the curves corresponding to different magnitudes for all models in this region start to converge.

Attenuation curves in subduction zones can be described as having wider range of applicability for distance. Based on Figure 3.5, at large magnitude and small distances, the predicted values of PGA are essentially independent of magnitude for models by CR91, PT04 and FT91, while the PGA at small distance predicted by AB97a and MW05 models are strongly dependent on magnitude. MW05 gives a very high PGA, i.e., higher than 1g, for a magnitude 9.0 earthquake.

As stated in the previous section, each model caters for specified ranges of

applicability established based on the database used in regression analysis. With this in mind, the use of these equations should be restricted to such prescribed ranges as the model may underestimate or over-predict the probable ground motions outside this limit. Conversely, this should not be the deciding factor in choosing the suitable model for a certain region. An attenuation relation may not be able to provide good approximation beyond its applicable range but measured ground motion records may still correlate significantly well when compared with its predicted values.
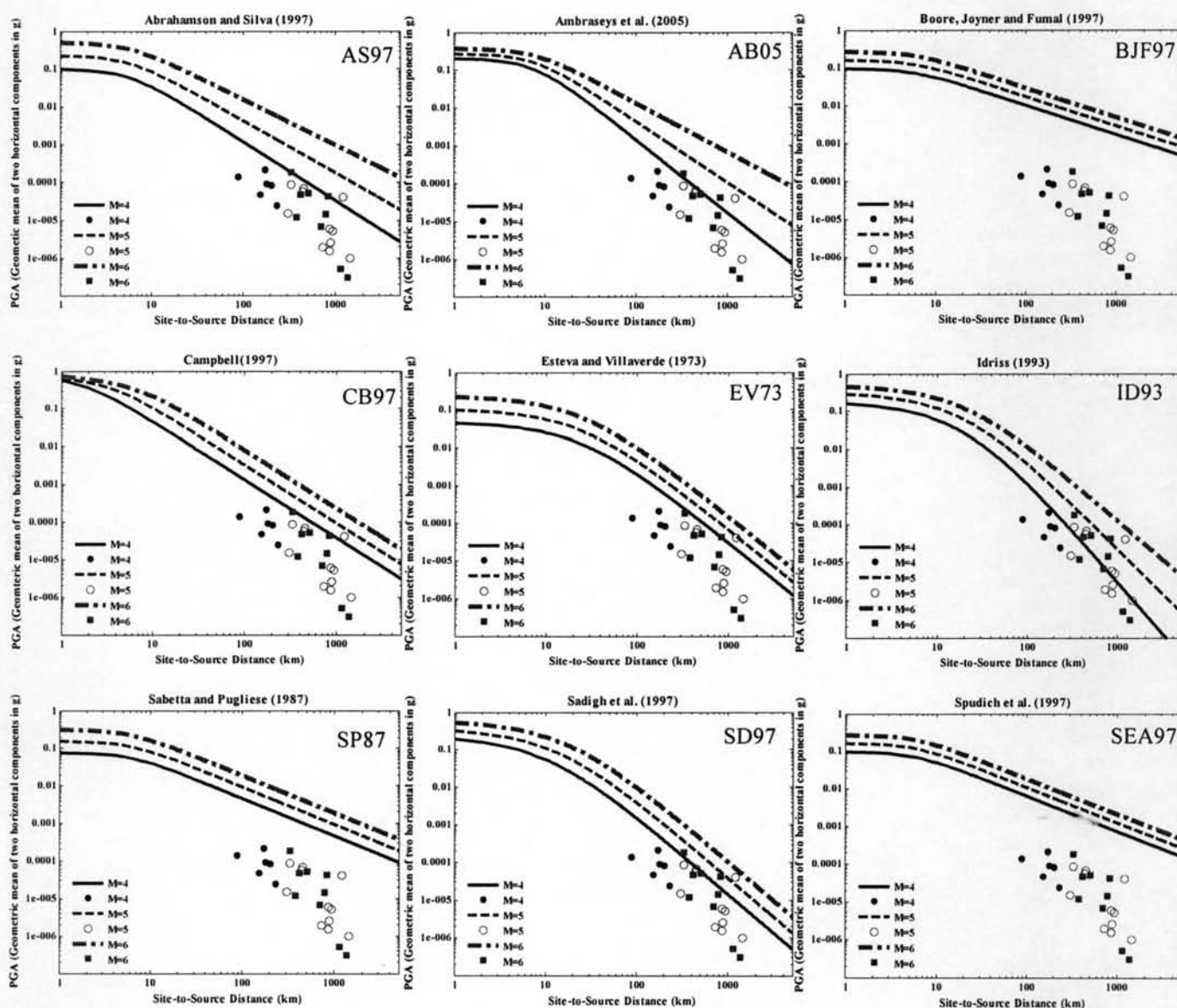
Figure 3.3 Attenuation curves of PGA for rock sites in active tectonic regions
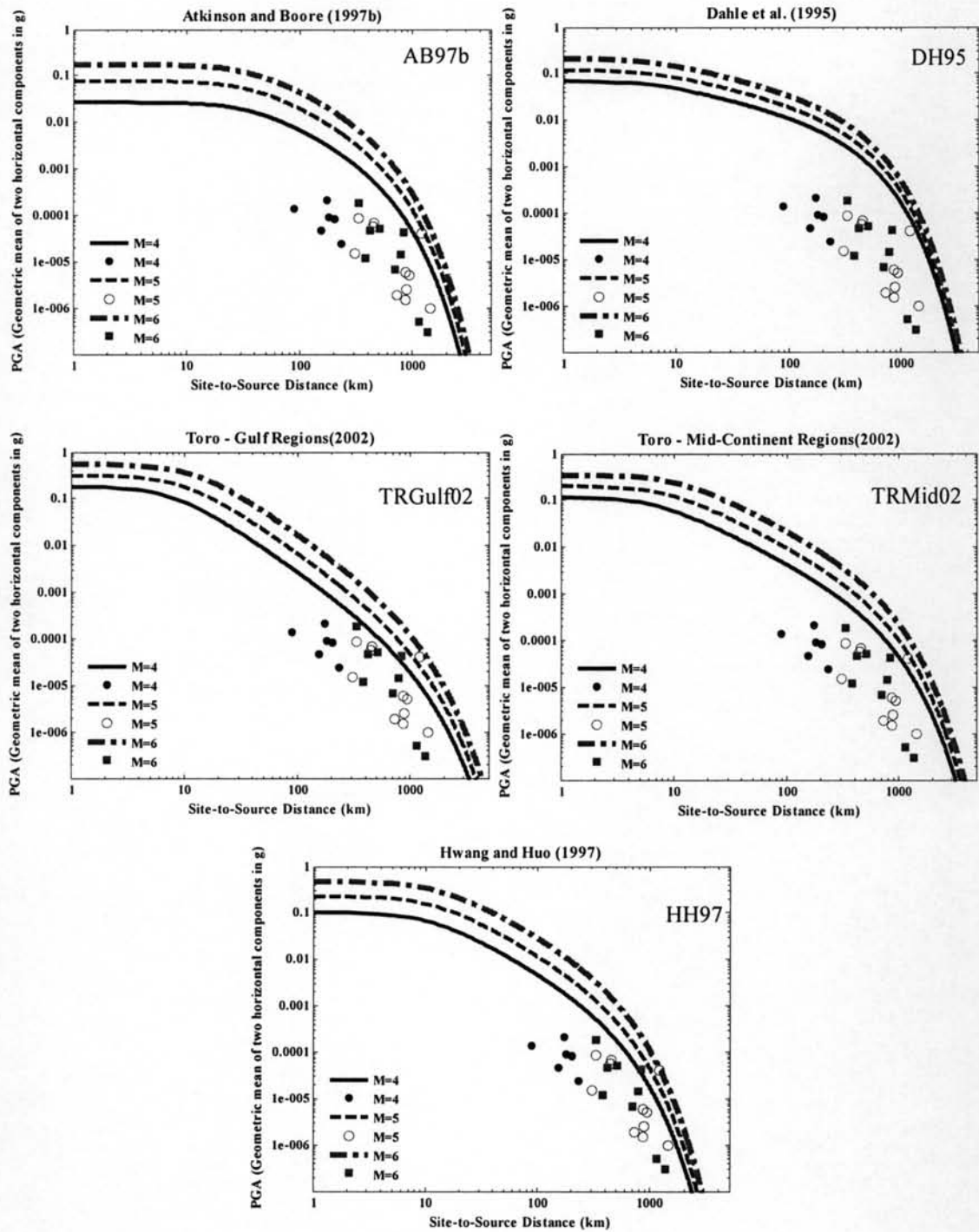
Figure 3.4 Attenuation curves of PGA for rock sites in stable continental regions
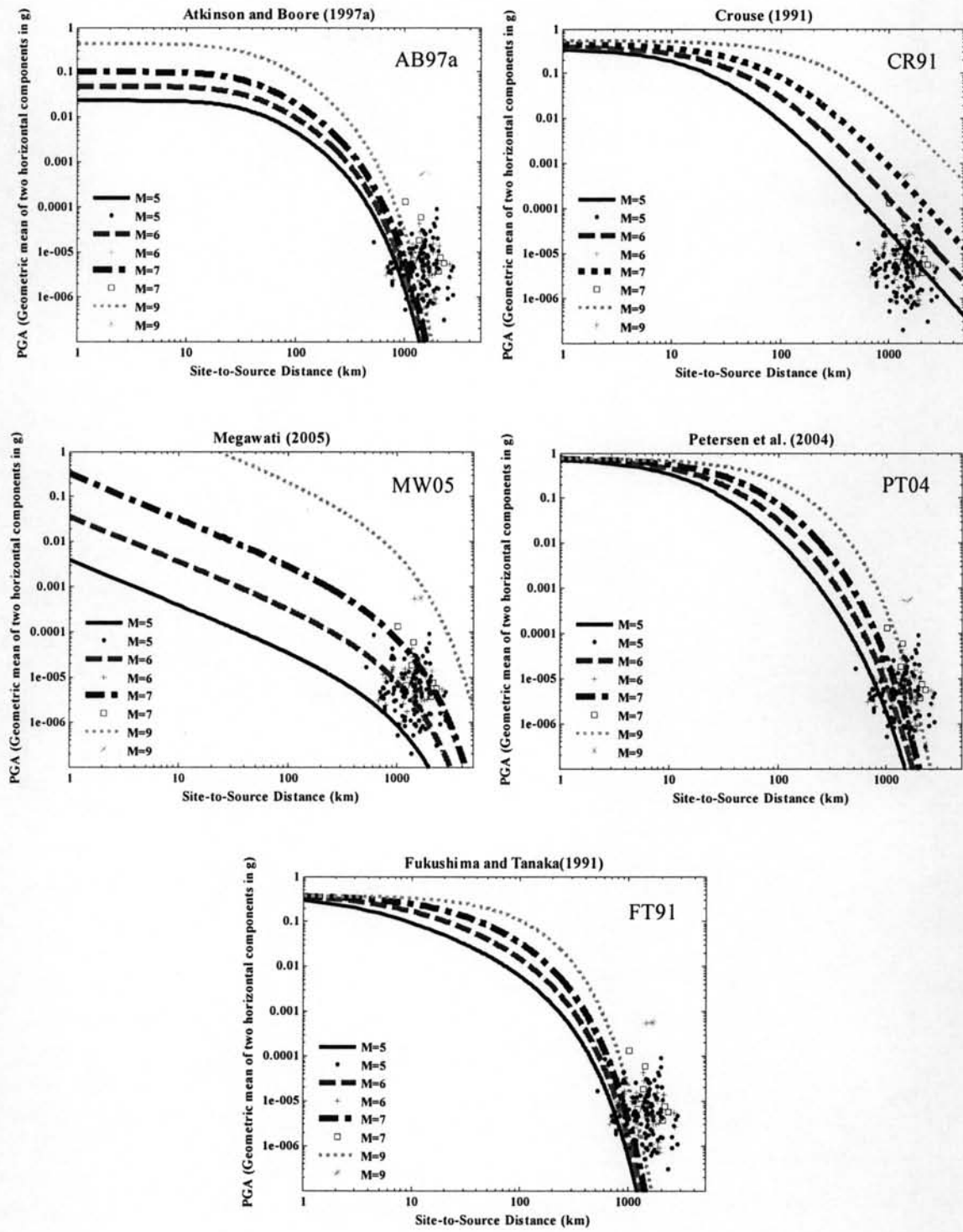
Figure 3.5 Attenuation curves of PGA for rock sites in subduction zones
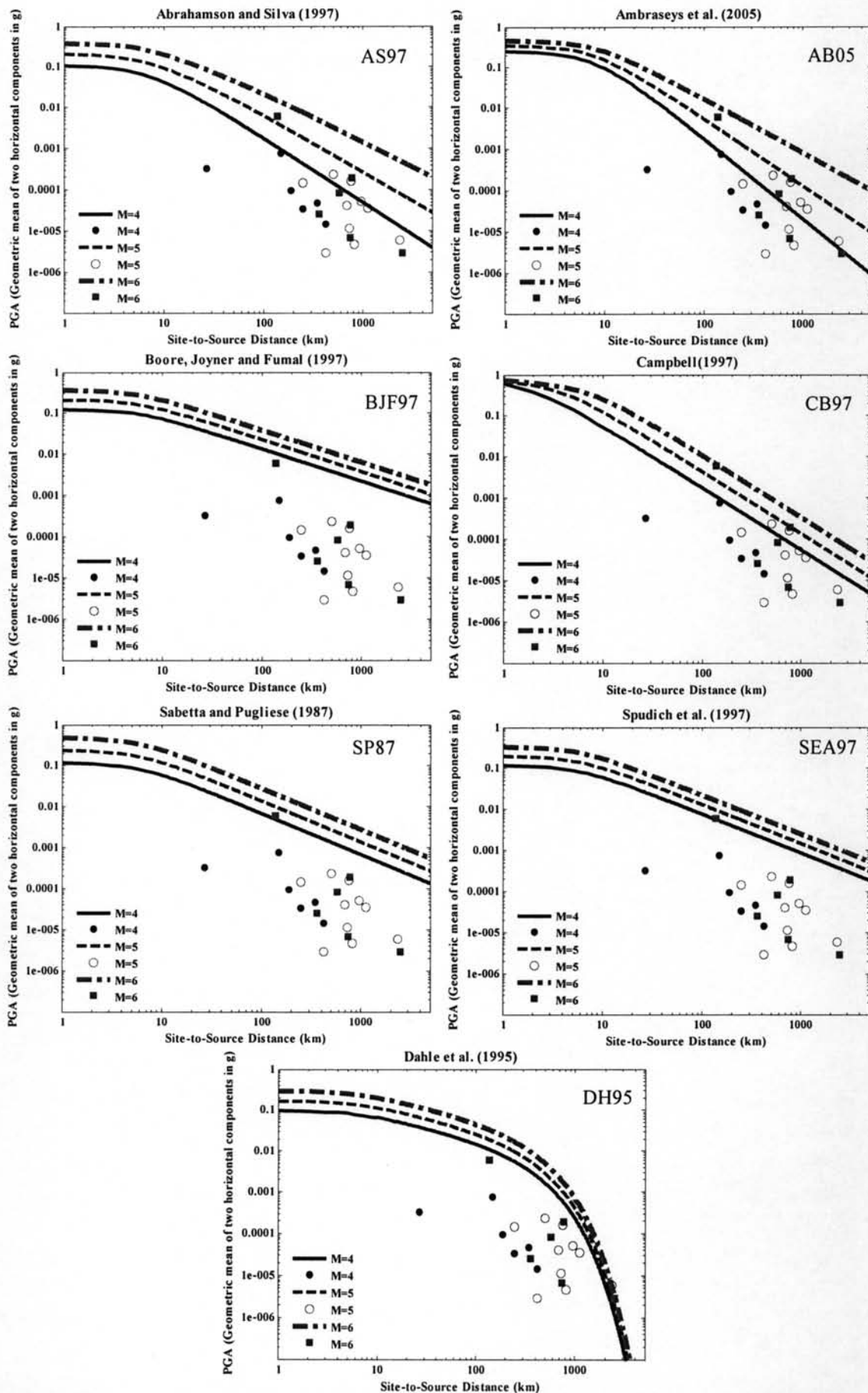
Figure 3.6 Attenuation curves of PGA on soil sites for non-subduction models
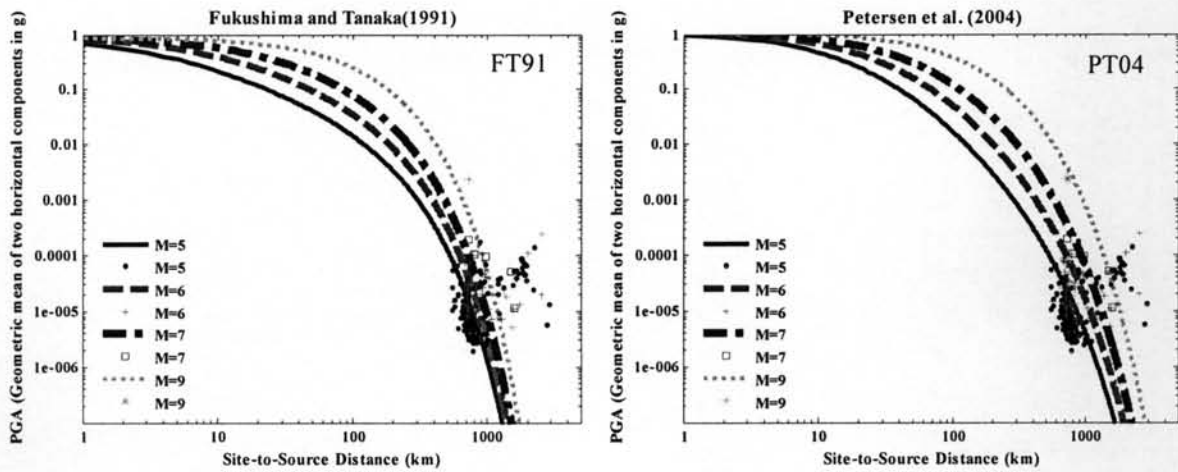
Figure 3.7 Attenuation curves of PGA for soil sites in subduction zones

To quantify the adequacy of the models, the residuals, which is the difference between the actual and predicted values of ln Y is analyzed by computing the square root of mean square of the residual (RMS) as given in Equation 3.22. This parameter reveals how closely the estimated values correspond to the actual field records.

$$RMS = \sqrt{\frac{\sum (\ln y - \ln \hat{y})^2}{n}} \qquad (3.22)$$

where

y   = actual data points;

$\hat{y}$ = predicted data points given by each attenuation model; and

n   = number of data points.

As a goodness-of-fit measure, RMS indicates how well an attenuation model predicts PGA according to the database. Smaller RMS indicates a better fit of the model to actual data. RMS values for each model are summarized in Table 3.8. Most of the models consider site category parameter in the prediction of ground motions. With that, both sets of rock and soil data are used as actual field PGA while the ground motions estimated by each model represent the predicted PGA values. Other models just take into account the prediction of ground motion at rock sites.

These computed RMS values are found to agree well with plots of attenuation curves. Models proposed by Idriss (1993) and Sadigh *et al.* (1997) for rock sites and Campbell (1997) and Ambraseys *et al.* (2005) for soil sites yield a relatively lower

RMS compared to other non-subduction models. For subduction zone models, Crouse (1991) and Megawati *et al.* (2005) for rock sites and Petersen *et al.* (2004) for soil sites provide a better fit.

Table 3.8 Summary of computed RMS using 1st data set

Attenuation Model	Rock Sites	Soil Sites
Active Tectonic Regions		
Abrahamson and Silva (1997)	3.71	3.08
Ambraseys *et al.* (2005)	3.40	2.67
Boore *et al.* (1997)	5.89	5.16
Campbell (1997)	3.09	2.54
Esteva and Villaverde (1973)	2.97	
Idriss (1993)	2.37	
Sabetta and Pugliese (1987)	4.93	4.33
Sadigh *et al.* (1997)	2.60	
Spudich *et al.* (1997)	5.17	4.38
Stable Continental Regions		
Atkinson and Boore (1997)	4.04	
Dahle *et al.* (1995)	4.62	5.16
Hwang and Huo (1997)	3.15	
Toro:Gulf Regions (2002)	3.07	
Toro: Mid-continent Regions (2002)	3.66	
Subduction Zones		
Atkinson and Boore (1997)	5.09	
Crouse (1991)	2.12	
Megawati *et al.* (2005)	2.64	
Petersen *et al.* (2004)	3.88	2.68
Fukushima and Tanaka (1991)	6.64	3.99

3.7   Effect of Focal Depth in Ground Motion Estimation

Attenuation relations that use focal depth as predictor variable in estimating ground motions are examined. The variation of focal depth with magnitude is shown in Figures 3.8 to 3.19 for these models. For equations in active tectonic regions and stable continental regions, a fictitious focal depth as a result of regression is usually specified while for subduction zone models, a value of 33 km is assumed. This value

represents the average focal depth of the data set used as well as the approximate value suggested by TMD.

In Figure 3.8 to 3.19, the focal depth at an increment of 5 km is varied within a small range of magnitude to compare the resulting estimate of ground motions with the field records which are grouped using a bin of 0.5 magnitude, ranging from a quarter of magnitude lower and a quarter of magnitude higher than the reference magnitude.

A general trend exemplified in the plots is that at an approximate site-to-source distance of 1 to 50 km, PGA decreases as focal depth increases in an amount that is constant at any magnitude input (Figures 3.8 to 3.16). Generally, this applies for the models in active tectonic regions as well as in stable continental areas although the difference in the generated PGA curves is more pronounced in the former than the latter. This discrepancy occurs at smaller level when compared to some subduction models as illustrated in Figures 3.17 to 3.19. However, for AB97a, the PGA curves decrease as values of focal depth increase as depicted in Figure 3.16. In addition, it is worthwhile to note that CR91 and PT04 yield similar PGA curves (Figures 3.17 and 3.19) at any focal depth input whereas MW05 (Figure 3.18) generates curves that changes with focal depth within the entire distance range.

A point worth highlighting is that based on the succeeding plots, the assumed value for focal depth does not influence the evaluation carried out for the candidate attenuation models since most of the data points do not fall within the distance range of 1 to 50 km. Hence, the results obtained using the database from TMD's digital stations before the 2006 system is unaffected by the variation of focal depth values. Had short-distance data points been available, then the effect of focal depth has to be considered in the assessment of attenuation models and other types of distance definition should be taken into consideration.
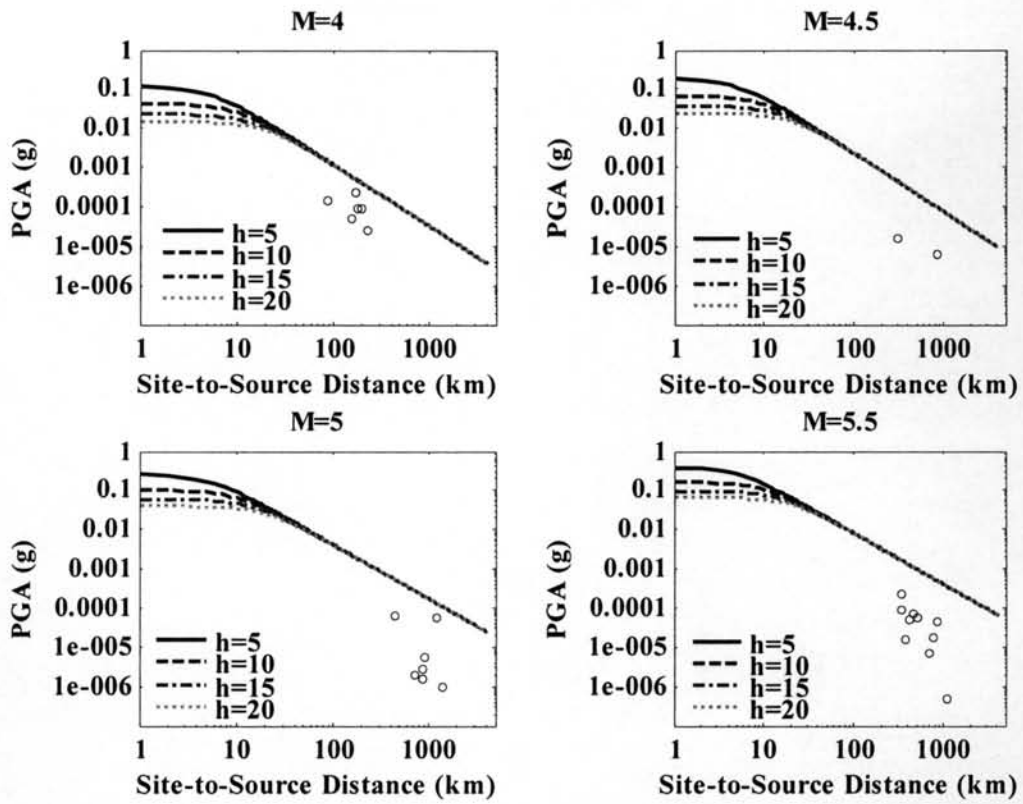
Figure 3.8 Abrahamson and Silva (1997)
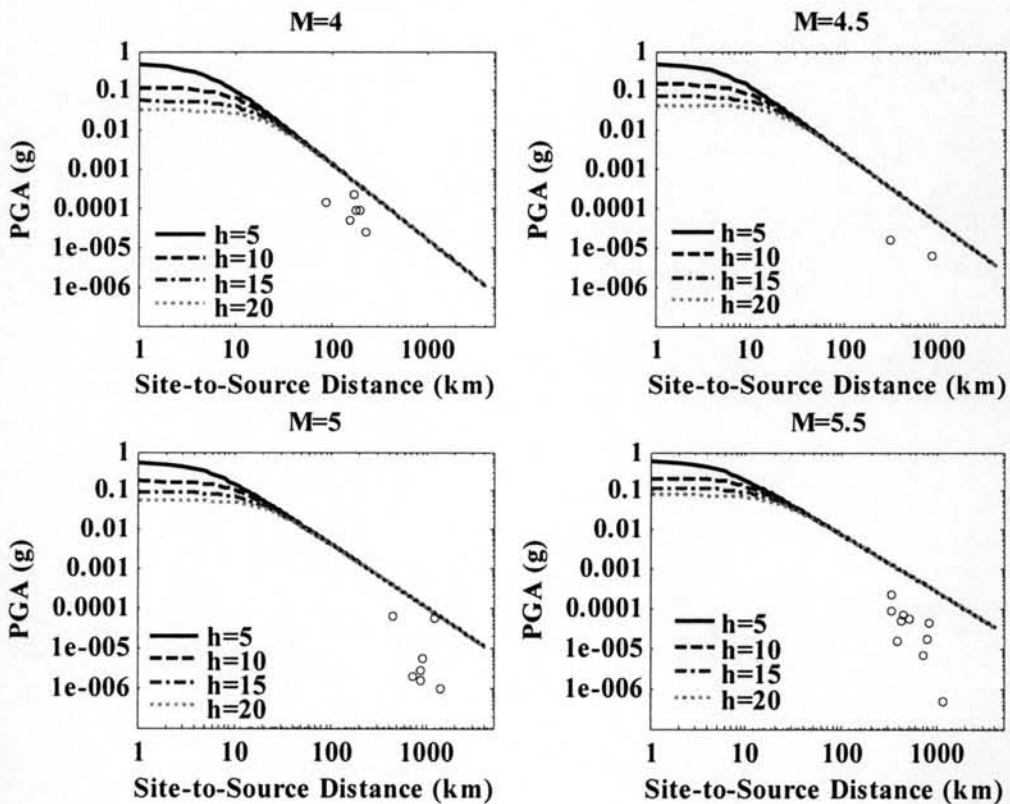
Figure 3.9 Ambraseys *et al.* (2005)
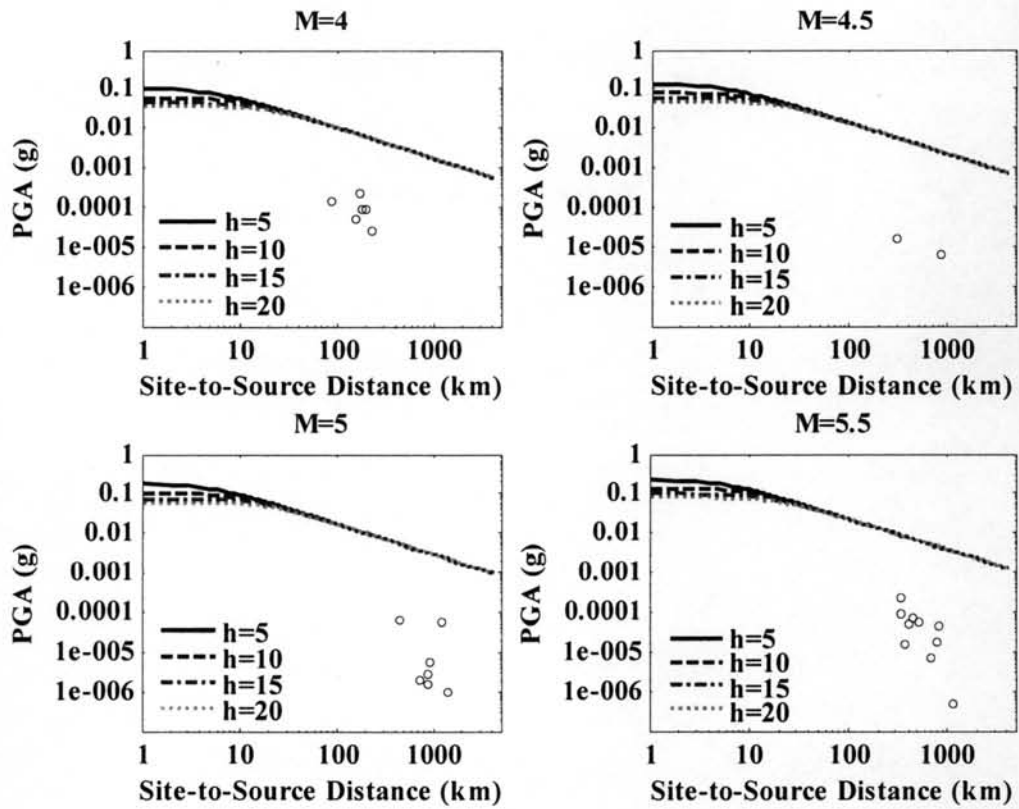
Figure 3.10 Boore *et al.* (1997)
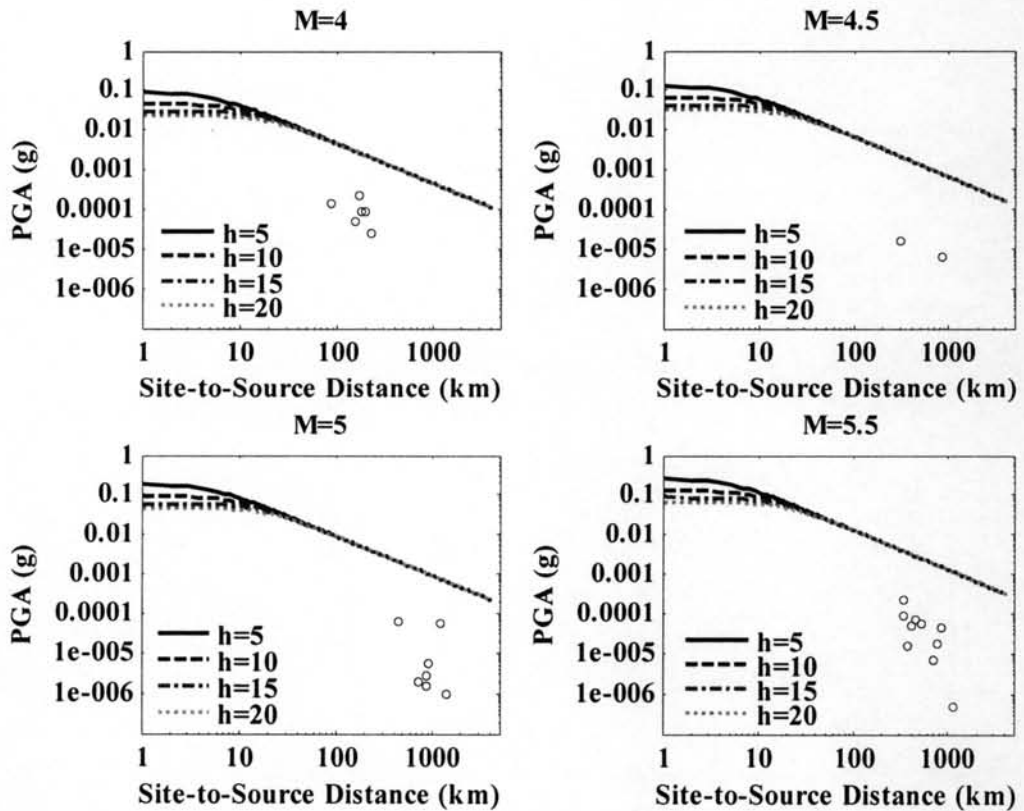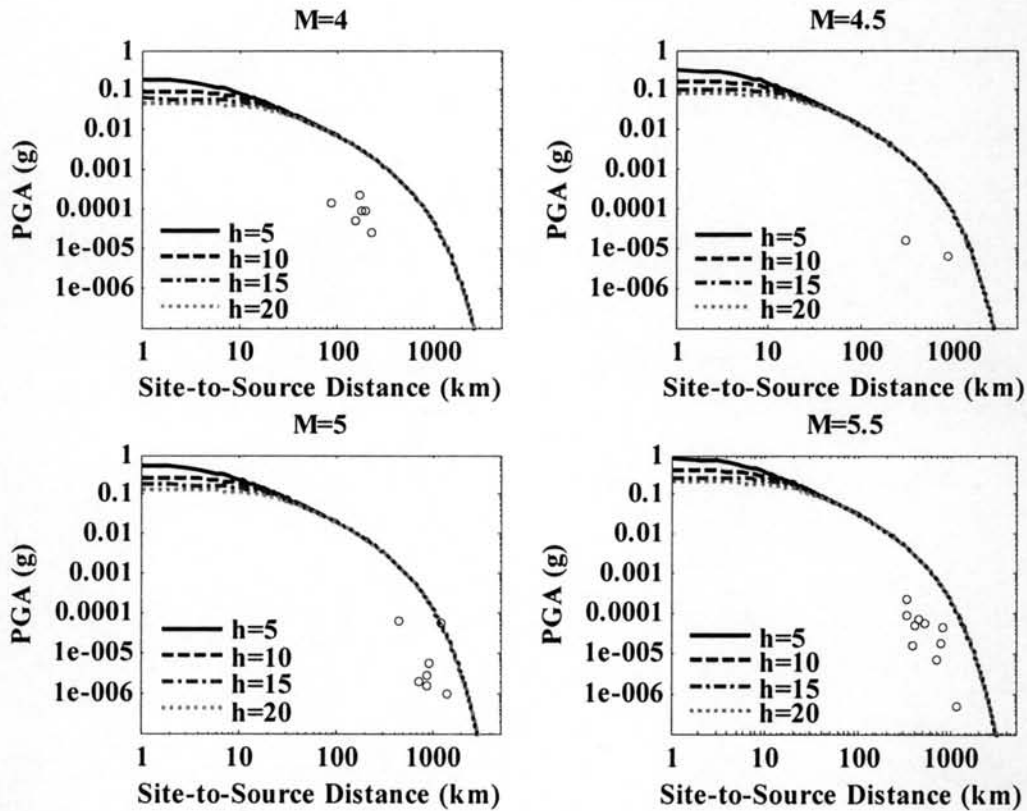

Figure 3.11 Sabetta and Pugliese (1987)
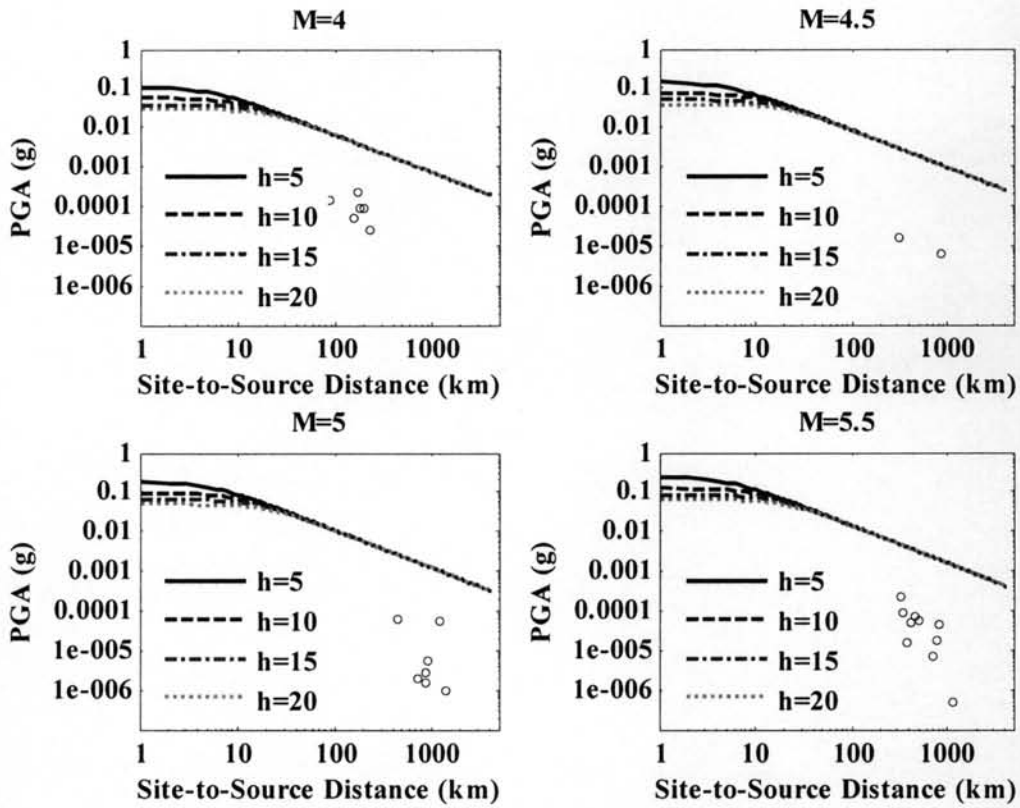
Figure 3.12 Spudich *et al.* (1997)

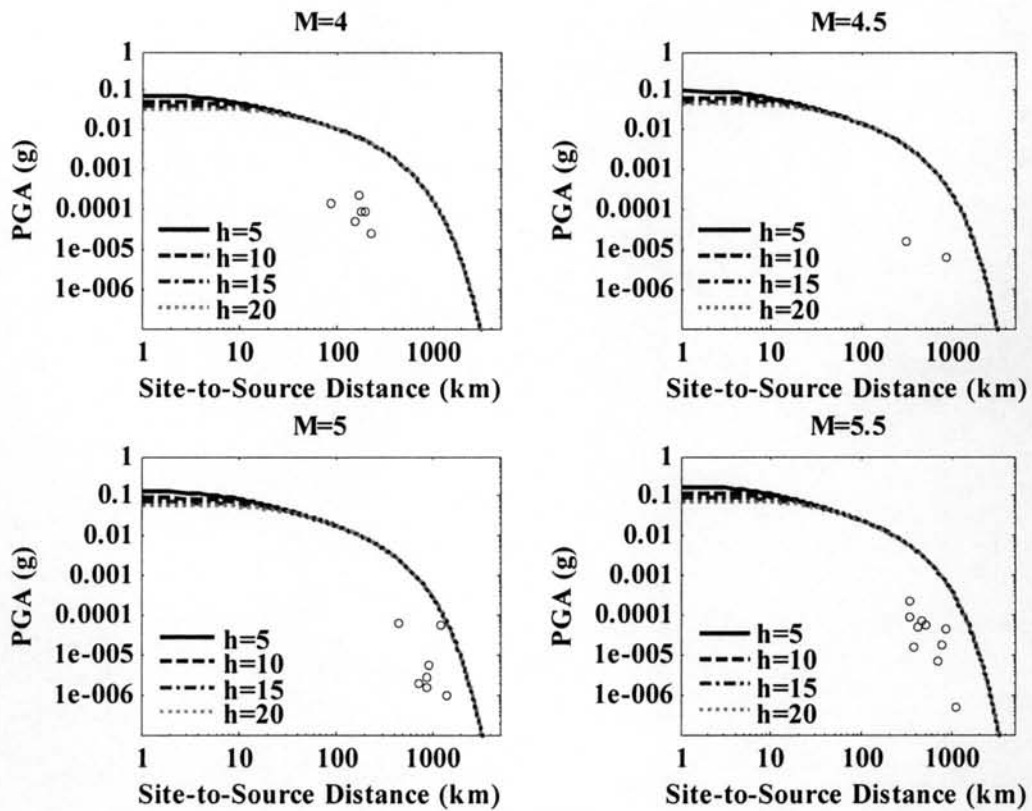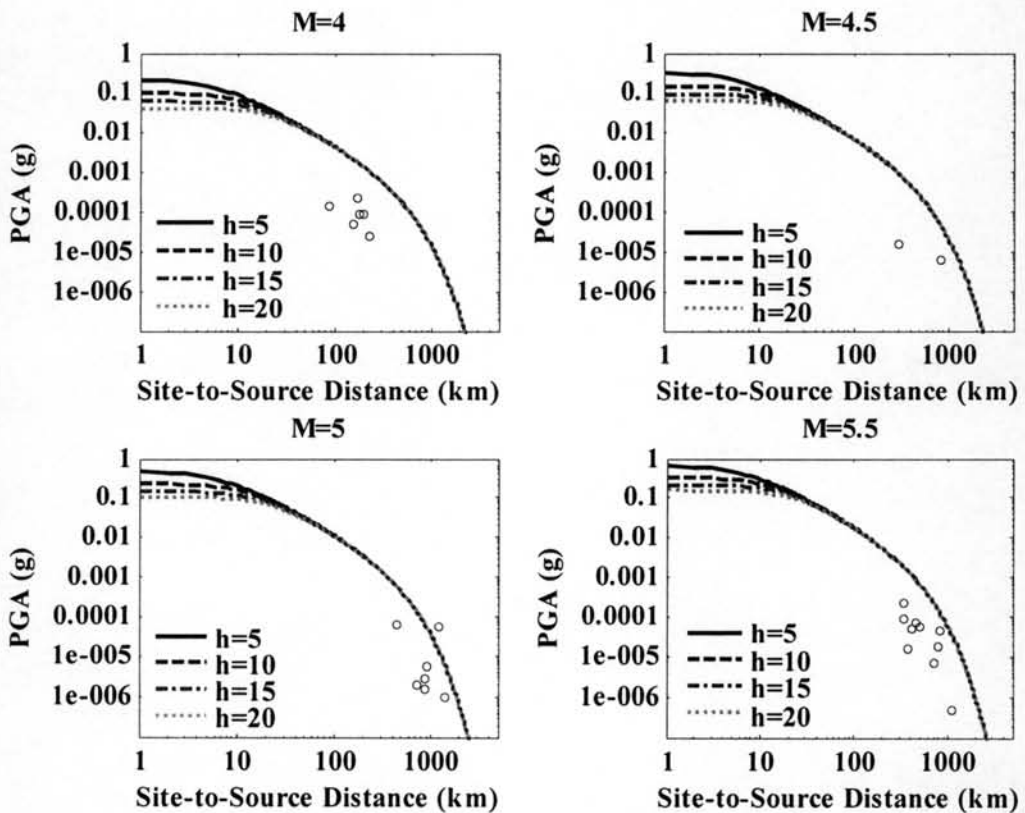Figure 3.13 Atkinson and Boore (1997b)

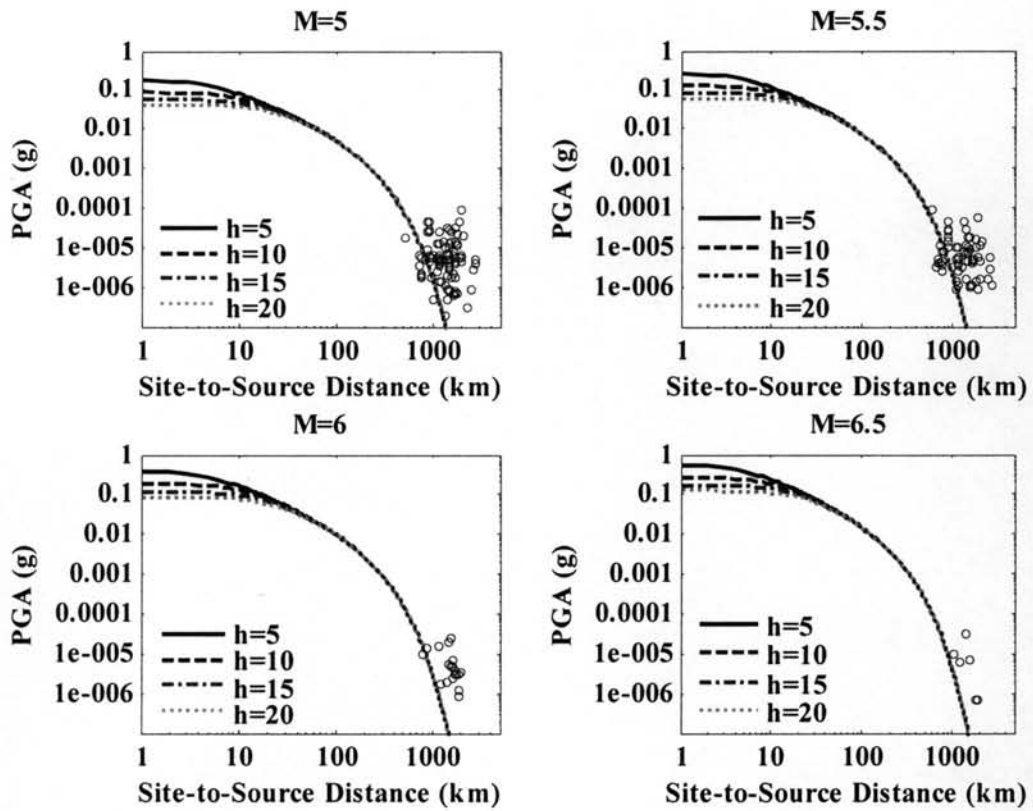**Figure 3.14 Dahle *et al.* (1995)**

Figure 3.15 Hwang and Huo (1997)

Figure 3.16 Atkinson and Boore (1997a)
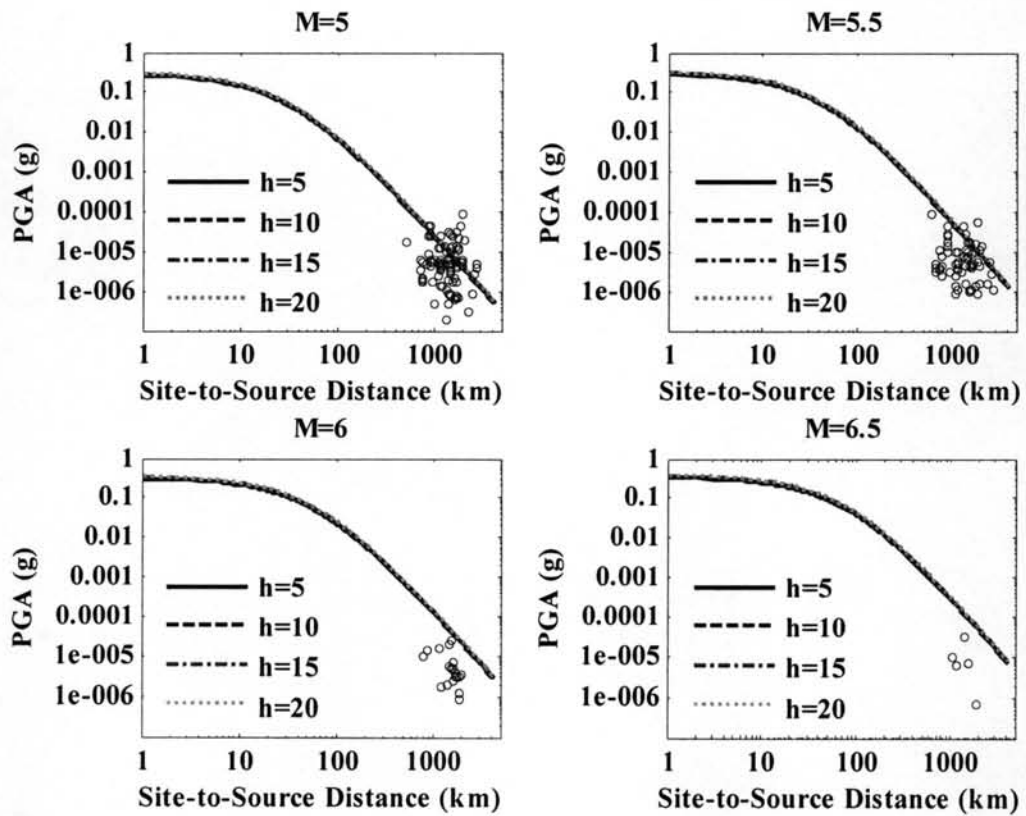
Figure 3.17 Crouse (1991)
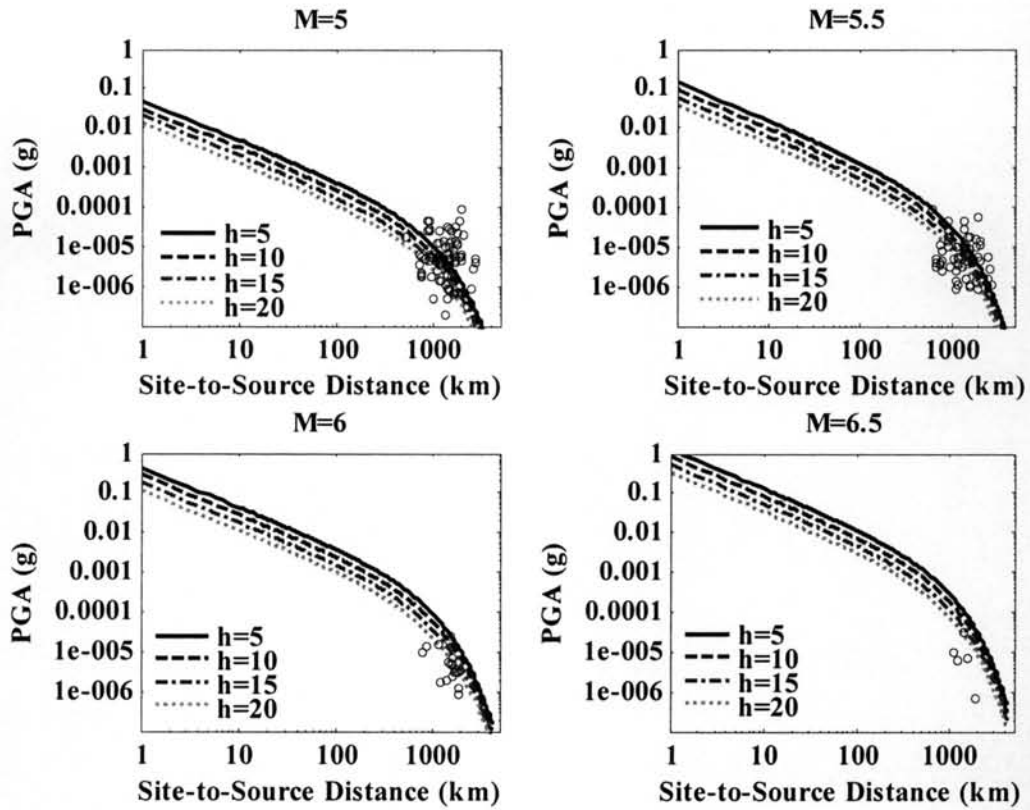
Figure 3.18 Megawati *et al.* (2005)
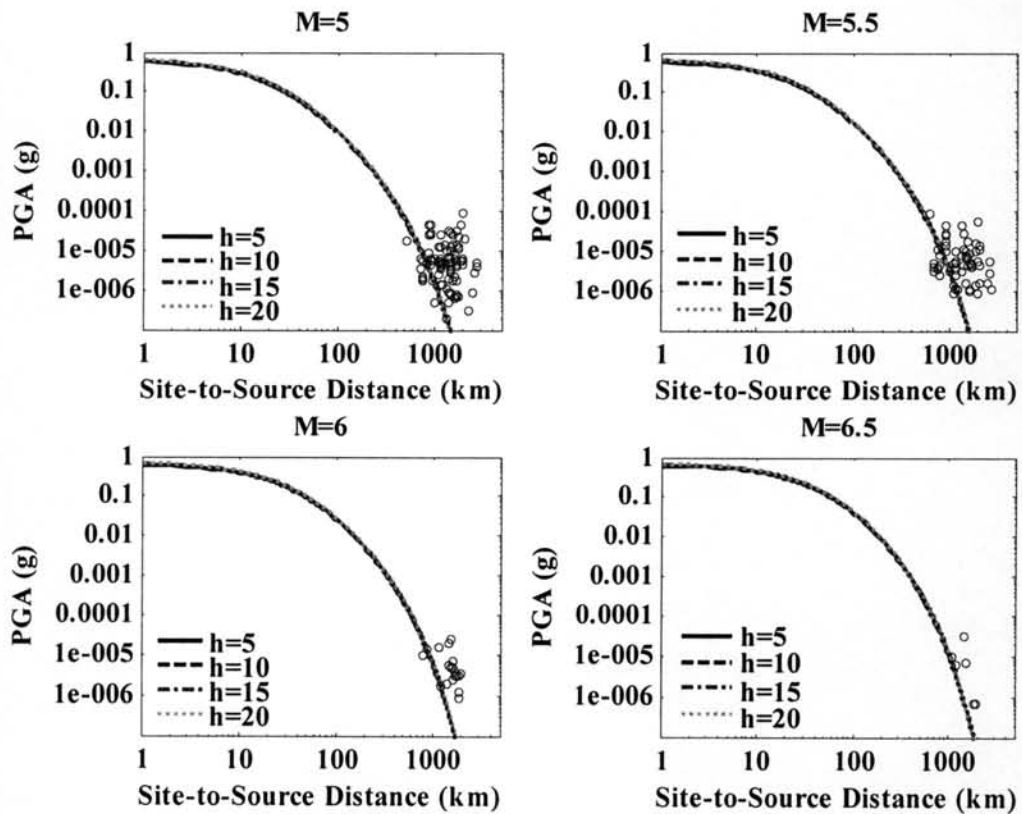
Figure 3.19 Petersen *et al.* (2004)

3.8   Comparison of Selected Attenuation Models to Data Set 2

Although the second data set is comprised of only 11 data points, valuable information can be collected by comparing these field records to the selected attenuation models using the same approach as presented in the previous section. The advantage of using these supplemental data is that the attenuation of seismic waves at various distances from the epicenter can be evaluated.

The limited number of data prompts an analysis that is not as comprehensive as the evaluation carried out for the first data set. Data points are calibrated to non-subduction zone models only since the epicenters of the events are situated on crustal regions. No distinction was made between rock and soil site classification as dictated by the small number of recordings.

As these data are compared to the attenuation models, the result shows consistency with the findings using the field records from TMD's old seismic stations. Attenuation curves for magnitudes 5.1 and 5.6 are plotted with 11 data points superimposed on each plot as shown in Figure 3.20 for models in active tectonic regions and Figure 3.21 for stable continental regions.

RMS is also computed for each model. Table 3.9 lists the RMS values corresponding to each model. The models of ID93 and SD97 have low RMS values and are found to correspond to the ground motion recordings of TMD's new digital seismic stations based on the attenuation curves generated. EV73 is also statistically robust and is able to represent the actual ground motions fairly well. However, more updated models, like ID93 and SD97, are available for use which can better represent the low attenuation properties of the region.

Shown in Figures 3.22 and 3.23 are the plots of the models which fit the data points considerably better than the other candidate models. The data points used for comparison are listed in Table 2.7. In these plots, Toro's (2002) model provide higher estimates of PGA compared with the other models which seem to cater for the low attenuation rates of the actual field records in Thailand. In addition, the models of EV73, ID93 and SD97 yield almost similar curves up to a distance of 100 km.

Note that suitable attenuation models for non-subduction earthquakes determined in this study were calibrated by using recorded data at distance ranging from 100 to 1000 km. Thus, these models are expected to give a good estimate of ground motions for this range of distance. They may not provide good estimates when distance is less than 100 km and attenuation models should be re-evaluated when more data at short distance become available.

Table 3.9 Summary of computed RMS using 2nd data set

| Attenuation Model	Rock Sites
Active Tectonic Regions	
Abrahamson and Silva (1997)	3.39
Ambraseys *et al.* (2005)	3.12
Boore *et al.* (1997)	5.26
Campbell (1997)	2.76
Esteva and Villaverde (1973)	2.62
Idriss (1993)	2.22
Sabetta and Pugliese (1987)	4.40
Sadigh *et al.* (1997)	2.35
Spudich *et al.* (1997)	4.58
Stable Continental Regions	
Atkinson and Boore (1997)	3.96
Dahle *et al.* (1995)	4.39
Hwang and Huo (1997)	3.10
Toro:Gulf Regions (2002)	2.81
Toro: Mid-continent Regions (2002)	3.43
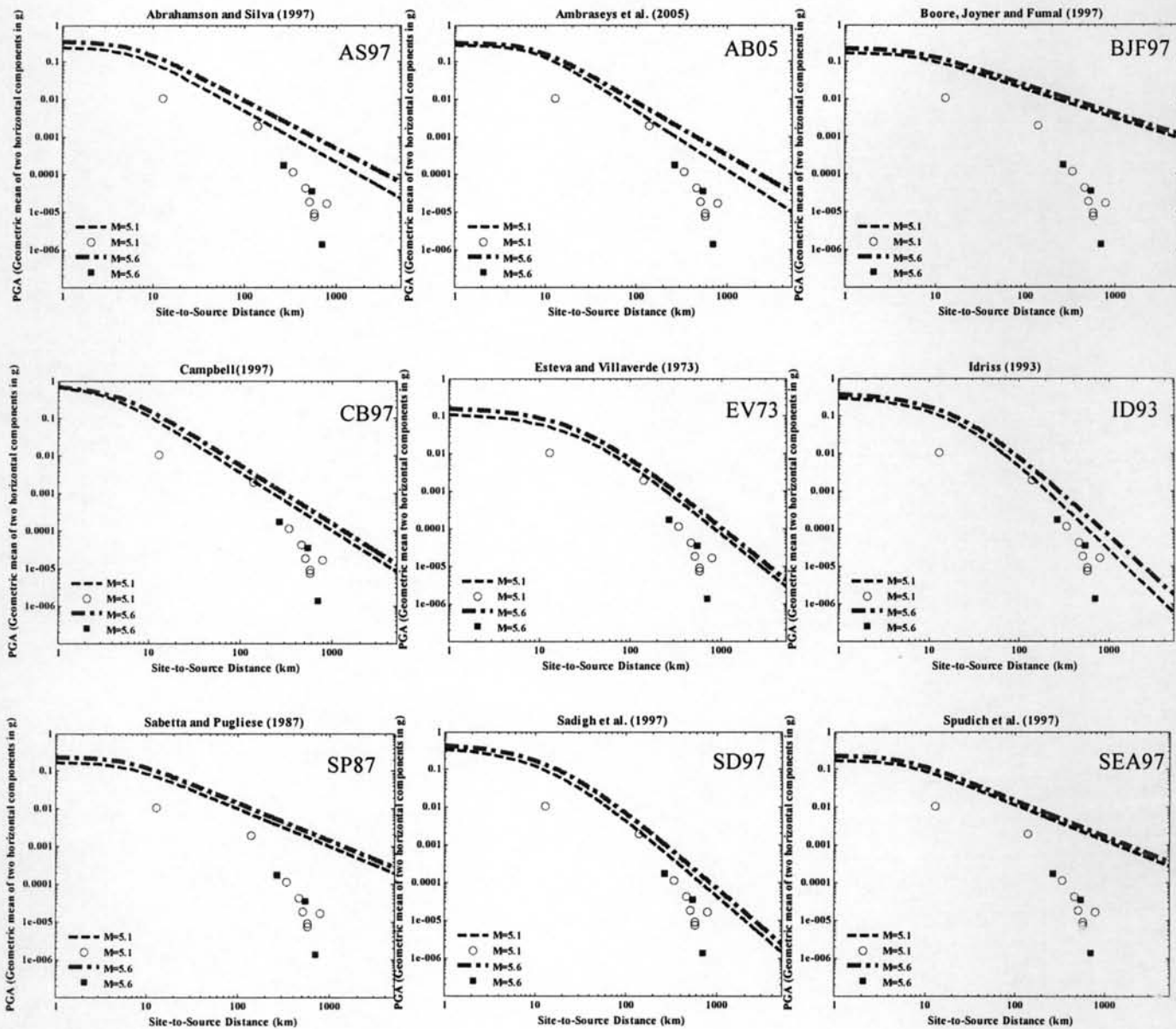
Figure 3.20 Comparison of attenuation models in active tectonic regions using field records from TMD's new seismic stations
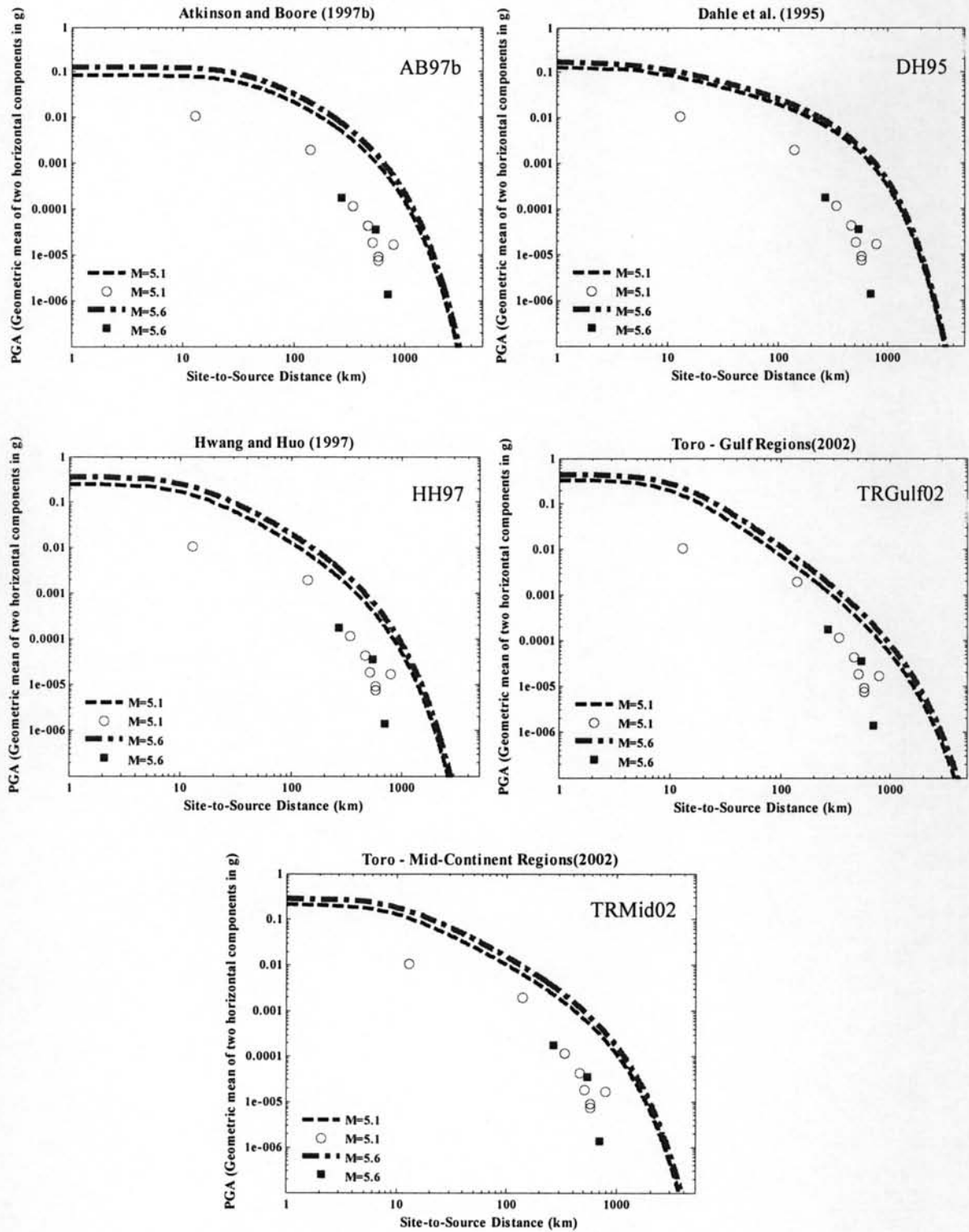
Figure 3.21 Comparison of attenuation models in stable continental regions using field records from TMD's new seismic stations
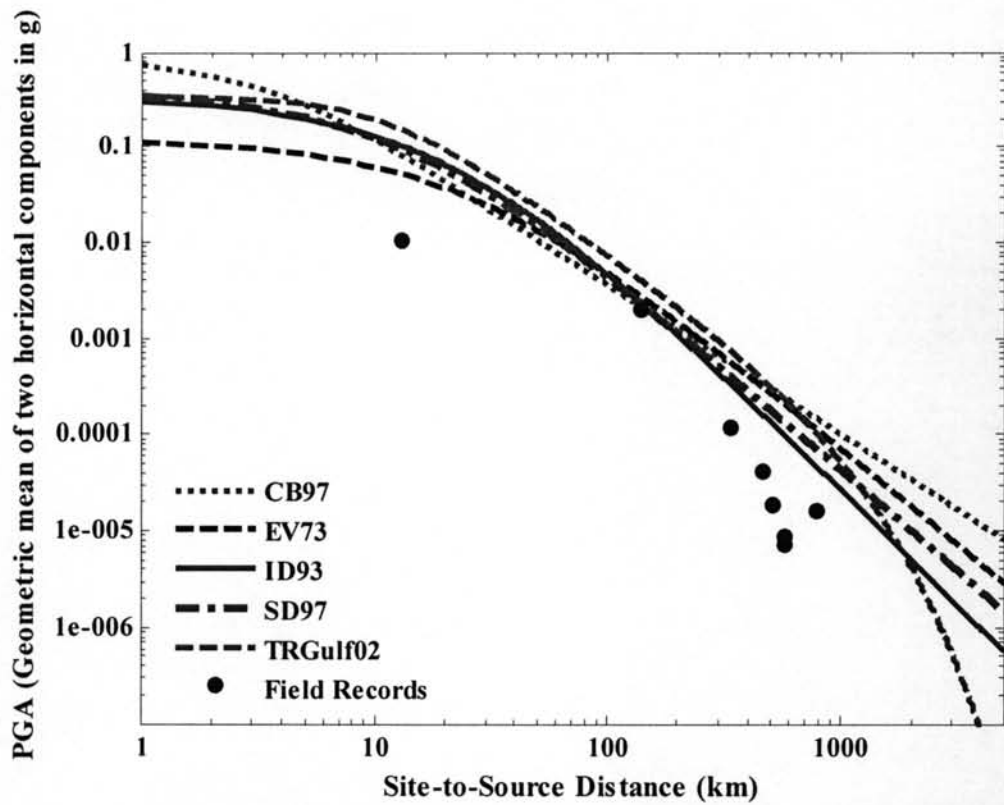
Figure 3.22 Comparison of selected attenuation models at M_L=5.1
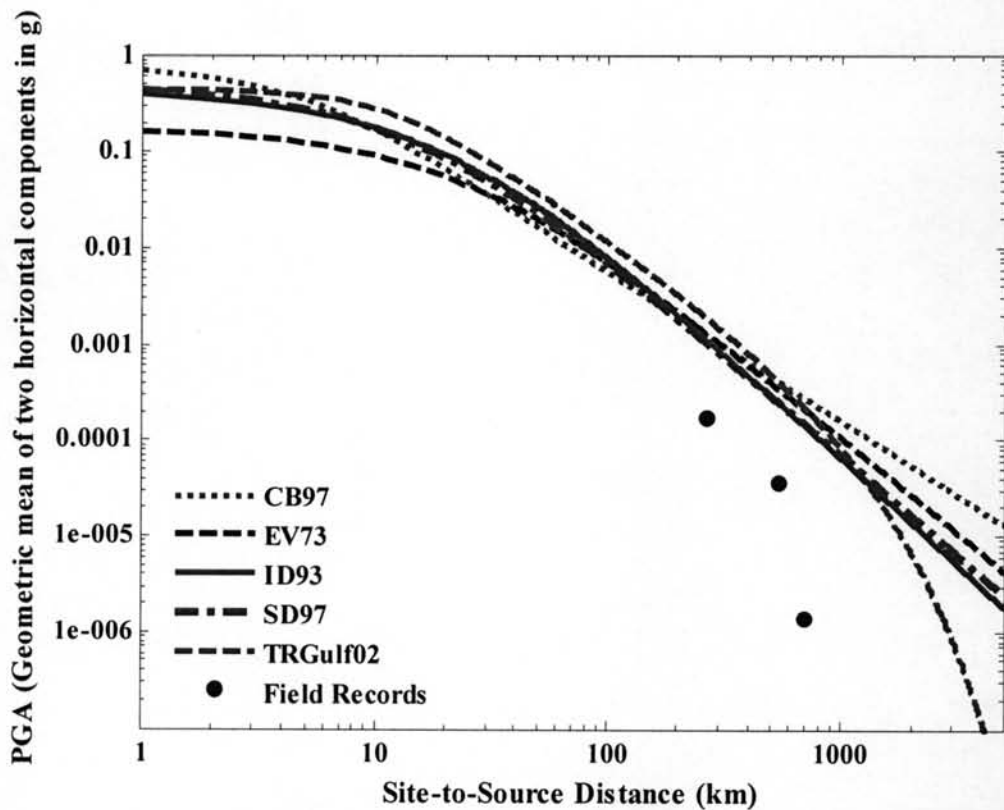
(December 13, 2006 Event at Mae Rim, Chiang Mai)

Figure 3.23 Comparison of selected attenuation models at M_L=5.6

(October 8, 2006 Event at Prachubkhirikhun)

It is evident from the plots shown above that the PGA measured by the recording instruments of TMD yield significantly low values compared with the estimated ground accelerations from the attenuation models. Moreover, slight structural damages (Figure 3.24) have been observed at a few houses in Mae Rim where the epicenter of the December 13, 2006 earthquake is situated while PGA values reported by TMD are about 1%g or less. Therefore, it is suspicious that the TMD seismic recording instruments maybe giving PGA lower than the actual values.
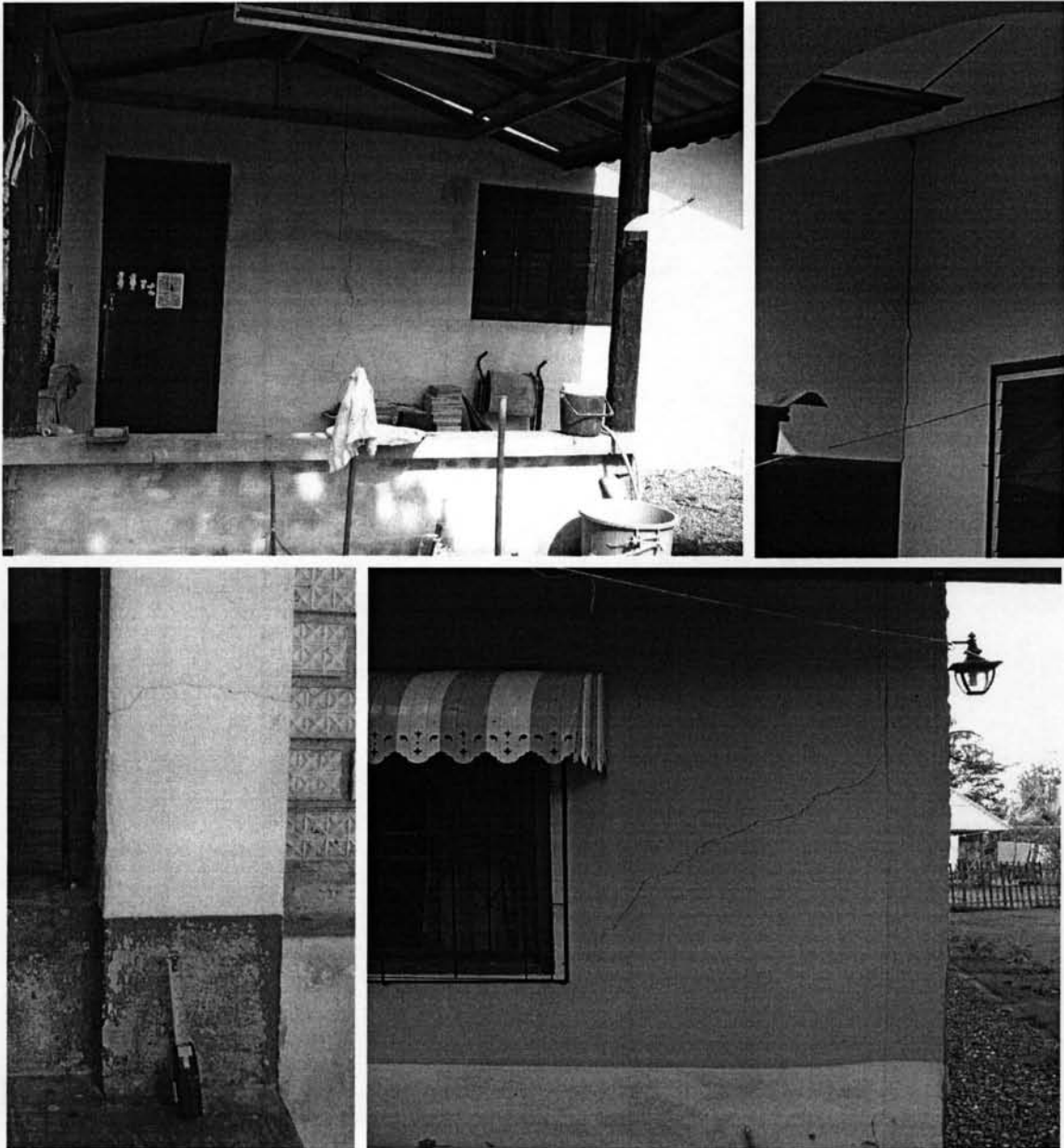

Figure 3.24 The damage caused by Mae Rim earthquake in December 2006